



# Active rifting and bimodal volcanism in Proterozoic Papaghni sub-basin, Cuddapah basin (Andhra Pradesh), India

SUKANTA GOSWAMI<sup>1,\*</sup>, SUKANTA DEY<sup>2</sup>, SYED ZAKAULLA<sup>1</sup> and M B VERMA<sup>3</sup>

<sup>1</sup>*Atomic Minerals Directorate for Exploration and Research, Bengaluru 560 072, India.*

<sup>2</sup>*IISER Kolkata, West Bengal 741 246, India.*

<sup>3</sup>*Atomic Minerals Directorate for Exploration and Research, Hyderabad 500 016, India.*

\*Corresponding author. e-mail: [sukantagoswami.amd@gov.in](mailto:sukantagoswami.amd@gov.in)

MS received 2 April 2019; revised 8 July 2019; accepted 8 August 2019; published online 20 December 2019

Bimodal volcanism in the Cuddapah basin is associated with a cratonic rift setting. The Cuddapah basin consists of five sub-basins (viz., Papaghni, Nallamalai, Srisaïlam, Kurnool and Palnad) and a total thickness of ~12 km sediments and associated bimodal volcanics. The oval-shaped gravity high observed over the Papaghni sub-basin is due to lopolithic intrusions along listric faults. A basin evolution model is prepared in this context with signatures of active rifting. Mapping and geochemical sampling along the Tadpatri–Tonduru tract along with petrographic observations additionally supports the proposed model. The model presents the mechanism of bimodal volcanism during rifting and sedimentation. Basin evolution with tectonic modifications revealed a link with global tectonic events (e.g., ~1.8 Ga Hudsonian orogeny, ~1.3 Ga Grenville orogeny, ~0.9 Ga Enderbia docking). The stratigraphic disposition of the surge, flow, fall and volcanoclastic deposits in this old Proterozoic terrane indicate the magma history and eruption conditions. The felsic volcanic rocks are classified as rhyolite and rhyodacite. The mafic volcanics are mainly basaltic. Primordial mantle normalized trace element plots indicate enrichment of large ion lithophile elements (Rb, Th and K) along with negative Sr, P and Ti anomalies. The chondrite normalized REE patterns are characterized by LREE enrichment, negative Eu anomaly and flat HREE pattern. These features indicate origin of felsic volcanics through shallow crustal melting with plagioclase either as a residual or a fractionating phase. The mafic rocks of the area are product of shallow mantle melting related to asthenospheric upwelling followed by decompression melting and generation of basaltic magma. This was also associated with lithospheric stretching, rifting and initiation of sedimentation. The less viscous mafic magma was probably channelized along the rift-related faults. The underplating and intraplating of hot mantle-derived magma supplied heat into the crust. The attendant partial melting of continental crust produced the felsic magma. Different sub-basins within the Cuddapah basin indicates a combined mechanism of rifting and orogenic events.

**Keywords.** Tectonics; bimodal volcanism; Cuddapah basin; Tadpatri Formation; volcanoclastics.

## 1. Introduction

Volcanic eruptions within sedimentary basins are often controlled by deep basinal architecture, basement faults and associated tectonics. Investigations on bimodal volcanic association have

significant implications for understanding formation and evolution of cratonic rift basins (Manatschal 2004; Koptev *et al.* 2016; Goswami *et al.* 2018; Goswami and Dey 2018). The role of rifting is significant in the formation of accommodation space and channelization of magma and heat flow

within the continental crust (McKenzie 1978; Manatschal 2004; Koptev *et al.* 2016). During the Proterozoic Eon voluminous clastic and chemical sedimentation took place in several cratonic basins in India over the Archaean basement. These Proterozoic basins are important archives of surface processes, volcanism and biological and atmospheric evolution that occurred over a prolonged period. The Archaean rocks of the Dharwar craton in south India form the basement of three such basins, i.e., Cuddapah, Bhima and Kaladgi (figure 1). The Cuddapah basin is located in the eastern part of the Dharwar Craton and hosts ~12 km thick succession of platform sediments exposed over 44,500 km<sup>2</sup> (Nagaraja Rao *et al.* 1987; Chatterjee and Bhattacharji 2001; Ramakrishnan and Vaidyanadhan 2008; Patranabis-Deb *et al.* 2012; Collins *et al.* 2015).

The crescent-shaped Cuddapah basin with less deformed western margin and intensively folded and thrustured eastern margin deserves attention. The five sub-basins (viz., Papaghni, Nallamalai, Srisailam, Kurnool and Palnad) within the basin are genetically linked. The earliest formed Papaghni sub-basin comprises of a swarm of dominantly mafic intrusions in the SW (figure 2a, b).

The sub-elliptical Papaghni sub-basin outline is noteworthy and it is observed that infilling sediments have also been adjusted with gradual rotation of strike to follow the sub-elliptical outline of the basin margin (Goswami *et al.* 2016a). Interestingly, the trends of mafic bodies are parallel to the strike of bedding planes. Papaghni sub-basin periphery from north to south shows systematic changes in bedding strike which is NE–SW in the northern part followed by NW–SE in the middle and ENE–WSW to E–W in the southern extreme. The mafic igneous emplacements of the Tadpatri Formation are studied by several workers. However, the associated felsic volcanic rocks have received little attention. The geochemical and geochronological data of the mafic igneous emplacements are more numerous than the felsic volcanic rocks (GSI 1981; Murty *et al.* 1987; Bhaskar Rao *et al.* 1995; Anand *et al.* 2003; French *et al.* 2008; Chakraborty *et al.* 2016). According to Dasgupta *et al.* (2013), rifting within the Dharwar Craton is possibly related to these emplacements at around 1.90 Ga during opening of the Cuddapah basin. A detailed account of structural aspects especially about rift related paleostress conditions in Papaghni sub-basin may be found in

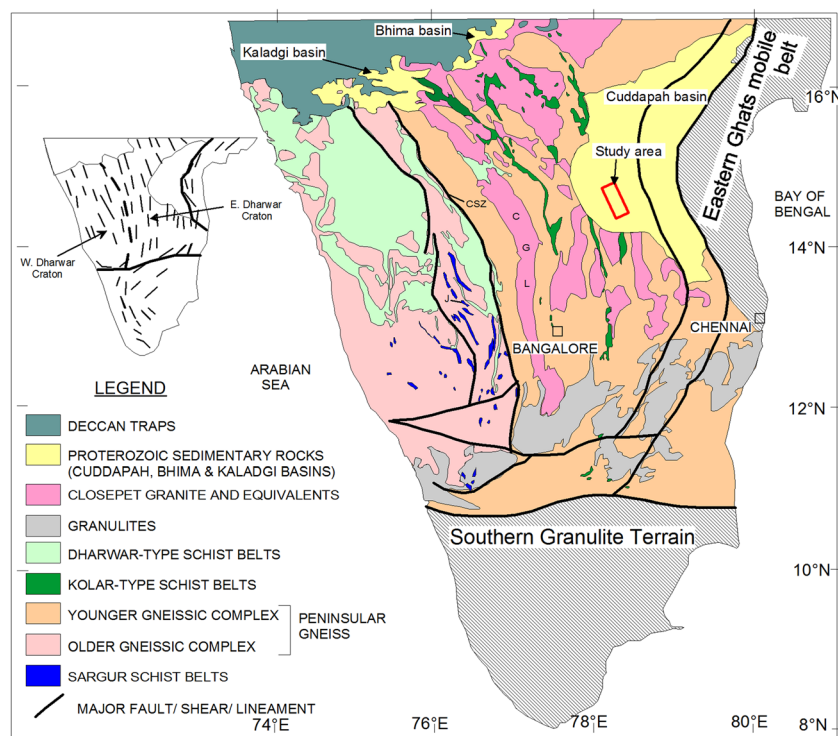


Figure 1. Geological map of the Dharwar craton, southern India (modified after Vasundhara Project, Geological Survey of India, 1994). CSZ: Chitradurga shear zone, CGL: Closepet Granite. The location of the Cuddapah basin and the study area for felsic volcanics are also shown.

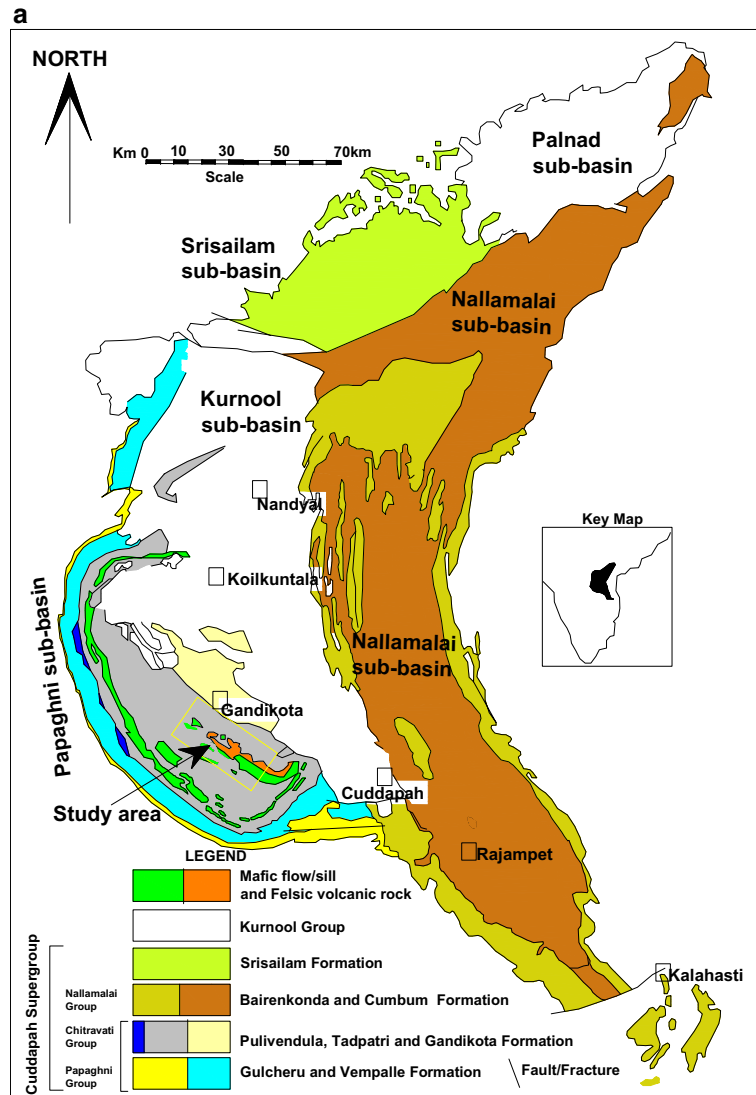


Figure 2. (a) Geological map of the Cuddapah basin (modified after Nagaraja Rao *et al.* 1987) showing different sub-basins. The rectangular block represents the study area. (b) Structural map of the Cuddapah basin (modified after Meijerink *et al.* 1984) showing the mafic igneous emplacements following the periphery of Papaghni sub-basin margin. Along the blue line, geological section (AB) was prepared by Geological Survey of India (1981) based on DSS profile data (Kaila *et al.* 1979). Anomalous structural areas are marked to indicate highly deformed and structurally complicated areas by Meijerink *et al.* (1984).

Tripathy and Saha (2013), Saha and Tripathy (2015) and Mukherjee *et al.* (2019).

Broadly E–W profile of about 100 km long Deep Seismic Sounding (DSS) across the basin was studied by Kaila *et al.* (1979, 1987) and presence of lopolithic structure in the basement up to about 5 km depth (figure 3a, b) was established in the Papaghni sub-basin (GSI 1981; Nagaraja Rao *et al.* 1987). Despite several remarkable literature availability (Chatterjee and Bhattacharji 2001; Anand *et al.* 2003; Halls *et al.* 2007; French *et al.* 2008; Ravikant 2010), the link between rifting and intrusion of such lopolith remained indeterminate. The mafic igneous rocks are studied with different objectives in some literatures (e.g., Chatterjee and

Bhattacharji 2001; French and Heaman 2010; Sesha Sai 2011; Belica *et al.* 2014; Chakraborty *et al.* 2016).

This work deals with the tectonic setting of the mafic igneous emplacements encircled inside the Papaghni sub-basin along with a thorough detailed analysis of felsic volcanics and tuffaceous volcanics in Tadpatri Formation. We have selected the best preserved outcrops and mapped (1:50,000 scale) the lava flows and tuffs (figure 4) over ~500 km<sup>2</sup> area. The spatial relationship between different volcanoclastic facies is recently recorded where several felsic volcanic textures are identified and discussed hitherto (Goswami *et al.* 2018; Goswami and Dey 2018). Several felsic volcanic textures are

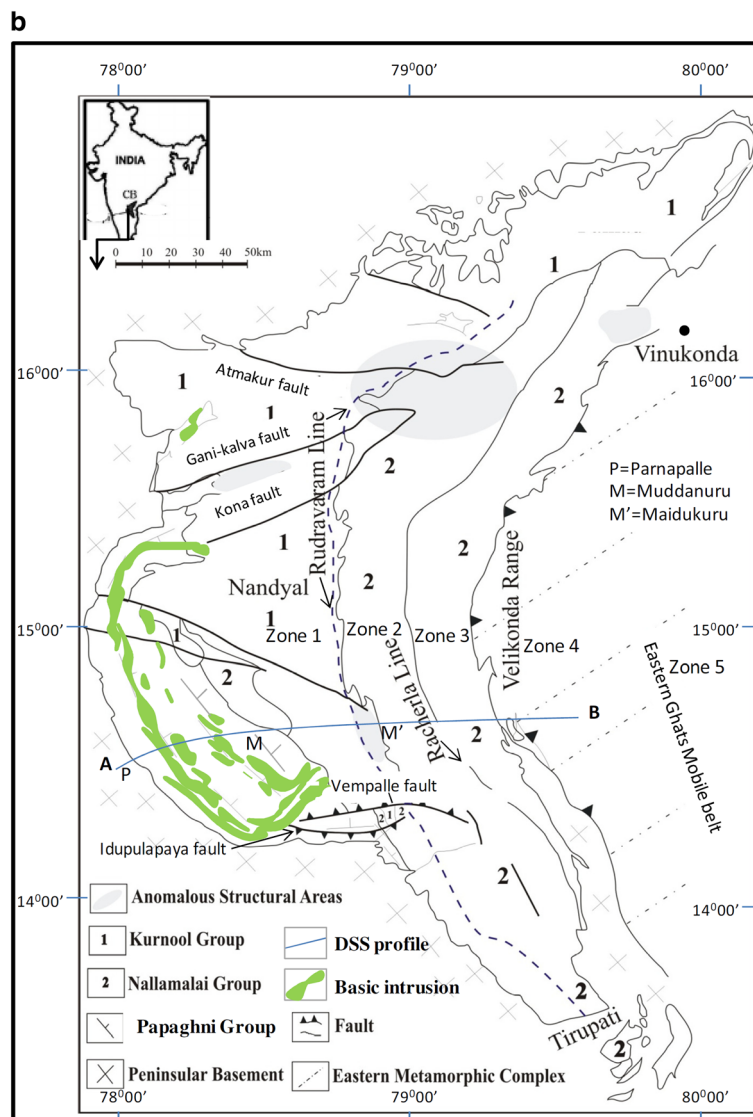


Figure 2. (Continued.)

identified and discussed for the first time with a systematic thin section studies under microscope and geochemical analysis of selected samples. The chemical composition of mafic and felsic volcanic and volcanoclastic rocks are used to interpret different aspects of magma history, viz., source of magma, evolution of magma and tectonic environment of magma eruption. The present work focuses mainly on the  $\sim 1.86$  Ga felsic volcanic rocks of Tadpatri Formation. Mafic igneous rocks of Tadpatri Formation are studied by different workers (Chatterjee and Bhattacharji 2001; Anand *et al.* 2003; Chakraborty *et al.* 2016; Sessa Sai *et al.* 2016).

For the global readers, this paper is relevant as a new insight into lopolith emplacement and rifting. The works after Walker (1966), Saemundsson (1979), Burchardt and Gudmundsson (2009) in the Iceland suggest similar approach where such a work can be

undertaken. The objective of the present work is set to address the following scientific issues:

How is the bimodal volcanism related with contemporary basin evolution?

What was the possible geodynamic process involved in volcanic eruption?

What was the possible mechanism of basin evolution?

## 2. Geological set-up

The Cuddapah basin in southern India extends for a length of about 445 km along the arcuate eastern margin with a mean width of  $\sim 100$  km. The basin is characterized by quartzite-shale-carbonate cycles and the early sediments of the basin are interspersed with volcanic flows and sills. The

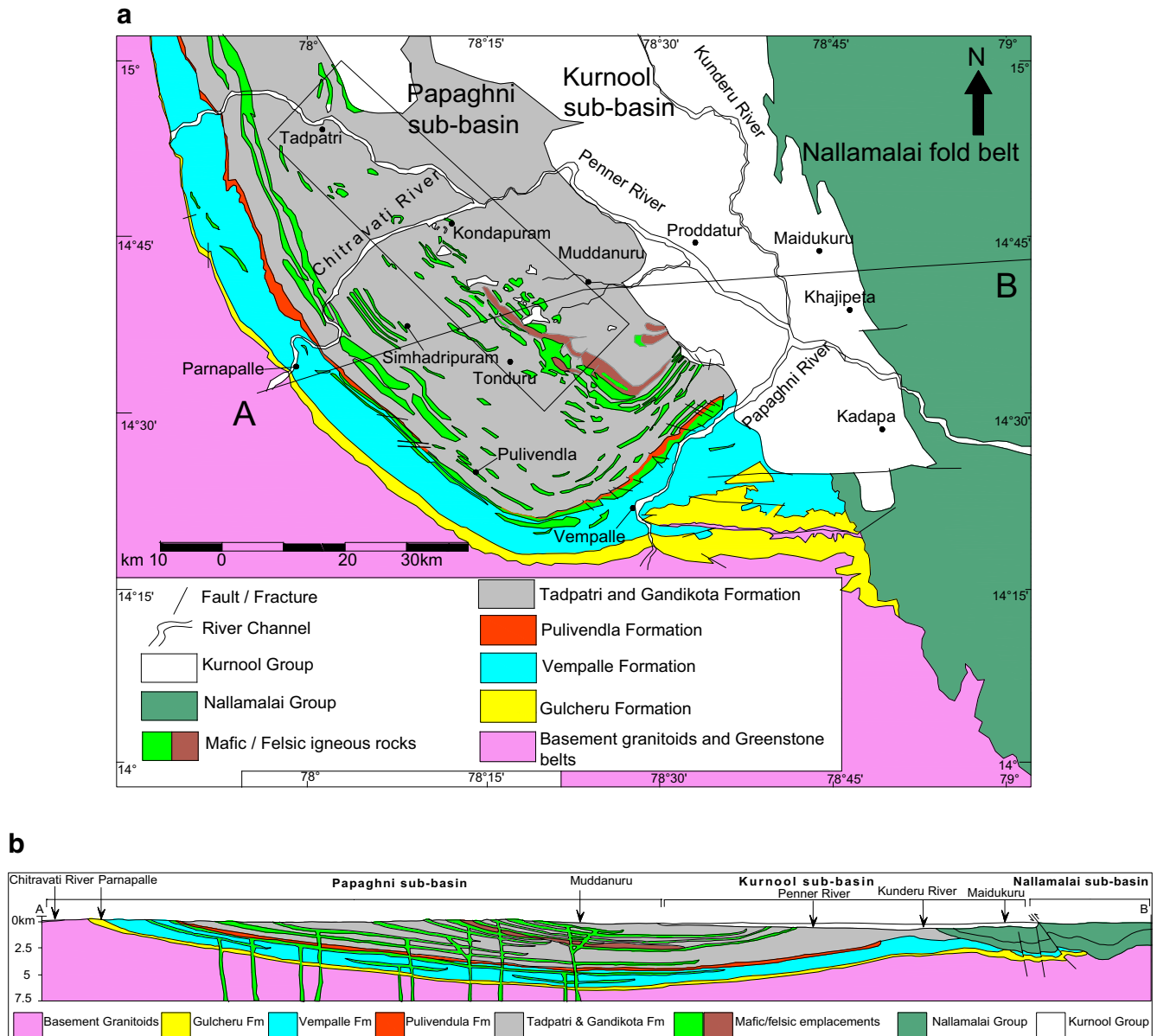


Figure 3. (a) Geological map of the SW part of Cuddapah basin showing the study area and surroundings with superimposed DSS profile line (after Geological Survey of India, 1981). (b) Geological section along the DSS profile line (Kaila *et al.* 1979) across the Papaghni sub-basin along Parnapalle–Muddanuru–Maidukuru tract (after Geological Survey of India, 1981).

arcuate eastern margin is deformed by a prominent thrust system (Nallamalai fold and thrust belt) which is parallel to the Eastern Ghats mobile belt and the East Coast of India (figure 1). The basin is nonconformably lying above the Archaean granitoids and greenstone belts of the East Dharwar Craton (EDC) in the north, south and west (Nagaraja Rao *et al.* 1987; Saha and Tripathy 2012; Patranabis-deb *et al.* 2012; Goswami *et al.* 2016a, b, 2017c; Mukherjee *et al.* 2019). The eastern margin of the basin is a tectonic margin along which metamorphosed Nellore schist belt rocks have been thrust up on the rocks of the Cuddapah basin. The rocks of Cuddapah basin are divided

into the Cuddapah Supergroup and the Kurnool Group. Stratigraphically, the Cuddapah Supergroup is divided into three groups, i.e., Papaghni, Chitravati and Nallamalai Groups (Nagaraja Rao *et al.* 1987; Lakshminarayana *et al.* 2001; Chaudhuri *et al.* 2002; Dasgupta and Biswas 2006; Chakrabarti *et al.* 2009; Saha and Tripathy 2012; Goswami *et al.* 2015, 2016c, 2017a, b, 2018; Goswami and Dey 2018). Table 1 shows the summary on stratigraphy, igneous episodes, available age data and mineral wealth of the Cuddapah basin. Cuddapah Supergroup of rocks occur in Papaghni, Nallamalai and Srisailam sub-basin. Kurnool Group occurs in Kurnool and Palnad sub-basins.

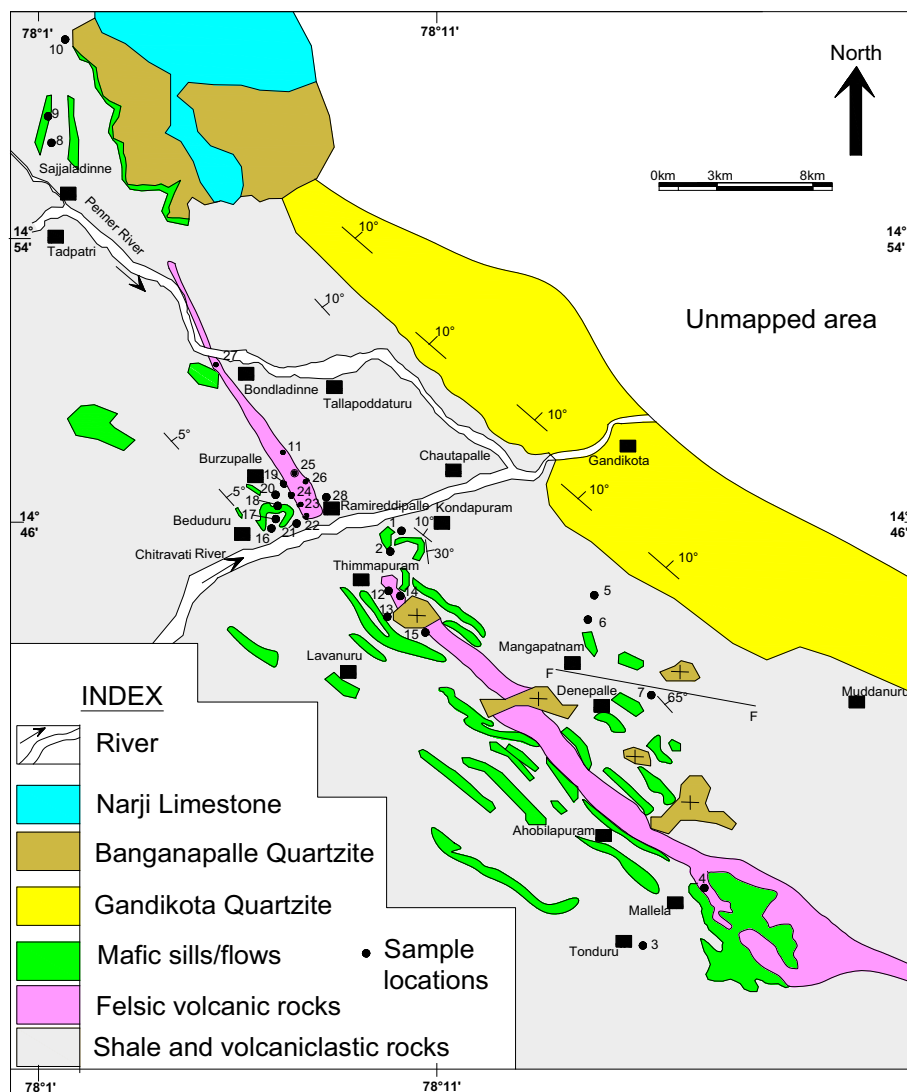


Figure 4. Geological map (this work) of the study area along Tadpatri–Tonduru tract showing sample locations.

The western part of the basin is relatively less affected by tectonic activity and sedimentary rocks dip gently ( $10^{\circ}$ – $15^{\circ}$ ). The rocks of Nallamalai Group in the east are intensely folded, with intensity and complexity of folding increasing from west to east. The Srisailam Formation in the Srisailam sub-basin occur unconformably on the Chitravati Group (Patranabis-Deb *et al.* 2012; Collins *et al.* 2015). The Neoproterozoic Kurnool Group unconformably overlies the Cuddapah Supergroup and represents two cycles of sedimentation depositing arenaceous-carbonate-shale sequence (Sharma 2011; Collins *et al.* 2015).

The bimodal volcanic emplacements and intrusive sills are most commonly observed in the Chitravati Group and also in the topmost portion of the Papaghni Group in the Papaghni sub-basin. Major igneous suites associated with the Vempalle and

Tadpatri Formations of Papaghni sub-basin are dolerite, picrite and gabbro sills, basaltic flows, felsic volcanic rocks, ignimbrites and ash fall tuffs. The Nagari/Bairenkonda Quartzite and Pullumpet/Curnbum Formations of the Nallamalai Fold Belt are traversed by dolerite sills (Karunakaran 1973, 1976; Dutt 1975; Nagaraja Rao and Mahapatra 1977; Deb and Bheemalingeswara 2008; Sesha Sai *et al.* 2017). Kimberlite dykes and syenite stocks are reported from the Curnbum Formation (Leelanandam 1980; Das and Chakraborty 2017). Exposures of granite/gneissic rocks with domal structures within the Curnbum Formation are variously interpreted as either intrusives into the sedimentary pile or reactivated portions of the basement gneisses.

Several workers have attempted to date the rocks of the Cuddapah basin (table 1). Table 2 represents a summary of age data within the Papaghni

Table 1. Composite log showing stratigraphy (after Nagaraja Rao et al. 1987) igneous events and mineral resources of the Proterozoic Cuddapah basin, southern India.

	Formation	Lithology	Thickness	Igneous activity	Isotopic Age	Minerals
K U R N O L  G R O U P	Nandyal Shale	Shale	50–100 m		913 ± 11 Ma (Detrital Zircon) <sup>H</sup> Maximum age	Limestone building materials
	Koilkuntla Limestone	Limestone	15–50 m			
	Paniam Quartzite	Quartzite	10–35 m			
	Owk Shale	Shale	10–15 m			
	Narji Limestone	Limestone	100–200 m			
	Banganapalle Quartzite <b>Angular unconformity</b>	Quartzite and Conglomerate	10–50 m			
C U D D A P A H  S U P E R G R O U P	Srisaigham Quartzite	Quartzite and Shale	~300 m			Uranium
	<b>Angular unconformity</b>  Cumbum (Pullampet) Shale	Shale/Phyllite Quartzite and Dolomite	~2000 m	Lamproite dykes, Syenite stock, Dolerite sills and Granite intrusives; Felsic volcanic rocks and tuffs	1418±8 Ma (Ar/Ar Phlogopite from chelima lamprolite) <sup>G</sup> , 1354±17 Ma and 1070±22 Ma (Rb/Sr Chelima and Zangamarajupalle Lamprolite respectively) <sup>F</sup> 1371±45 Ma (K/Ar chelima lamprolite) <sup>A</sup>	Barite, Pb, Cu, Zn
	Bairenkonda (Nagari) Quartzite <b>Angular unconformity</b>	Quartzite, Shale, Conglomerate	1500–4000 m	Dolerite sills		
	Gandikota Quartzite	Quartzite, Shale	~300 m			
	<b>Tadpatri Formation</b>	Shale, Tuff, Quartzite, Dolomite, Felsic and mafic volcanic rocks	~4600 m	Siliceous tuff and felsic volcanoclastics, Dolerite, Picrite and Gabbro sills and dykes, basaltic flows	1862±9 Ma U–Pb felsic volcanic rock (Zircon age) <sup>I</sup> , 1817±24 Ma (Rb/Sr mafic sill; whole-rock) <sup>E</sup> , 1899±20 Ma (Ar/Ar phlogopite from mafic sill) <sup>D</sup> 1756±29 (Pb/Pb age of U mineralisation and minimum age of dolomite) <sup>C</sup> 1885±3.1 Ma (U/Pb Beddeleyite from mafic sills) <sup>B</sup>	
	Pulivendla Quartzite <b>Disconformity</b>	Quartzite, Conglomerate	1–75 m			Uranium
	Vempalle Formation	Dolostone, Mudstone, Quartzite	~1900 m	Dolerite, Picrite and Gabbro Sill and Dykes, basaltic flow		Uranium, Asbestos, Barite
	Gulcheru Quartzite	Quartzite, Conglomerate	28–210 m	Dolerite dykes		Uranium

A: Murthy et al. (1987), B: French et al. (2008), C: Zachariah et al. (1999), D: Anand et al. (2003), E: Bhaskar Rao et al. (1995), F: Anil Kumar et al. (2015), G: Chalapathi Rao et al. (1999), H: Collins et al. (2015), and I: Sheppard et al. (2017).

Table 2. Geochronological data in and around Tadpatri Formation.

Rock type dated	Techniques applied	Age	Dated by
Felsic volcanic rock in Tadpatri Formation	U–Pb (SHRIMP) (Zircon age)	1862 ± 9 Ma	Sheppard <i>et al.</i> (2017)
Differentiated mafic sill of Tadpatri Formation	U–Pb IDTIMS (Baddeleyite age)	1885 ± 3.1 Ma	French <i>et al.</i> (2008)
Differentiated mafic sill of Tadpatri Formation	<sup>40</sup> Ar– <sup>39</sup> Ar (Phlogopite age)	1899 ± 20 Ma	Anand <i>et al.</i> (2003)
Mafic sill in Tadpatri Formation	Rb–Sr (Whole-rock)	1817 ± 24 Ma	Bhaskar Rao <i>et al.</i> (1995)
Mafic sill in Tadpatri Formation	K–Ar (Whole-rock)	958 ± 29 Ma	Murty <i>et al.</i> (1987)
Mafic sill in Pulivendula Formation	Ar–Ar (Whole-rock)	~1879 Ma	Chatterjee and Bhattacharji (2001)
Uranium bearing Vempalle Dolostone	<sup>206</sup> Pb– <sup>204</sup> Pb (Whole-rock)	1756 ± 29 Ma	Zachariah <i>et al.</i> (1999)
Mafic flow in Vempalle Formation	K–Ar (Whole-rock)	1841 ± 71 Ma	Murty <i>et al.</i> (1987)
Mafic flow in Vempalle Formation	Rb–Sr (Whole-rock)	1550 ± 147 Ma	Crawford and Compston (1973)

sub-basin. The youngest dated dykes in the basement showed Pb–Pb baddeleyite ages of  $2081.8 \pm 1.1$  Ma (Anil Kumar *et al.* 2015). The rocks of Cuddapah basin rest unconformably above such dykes. Therefore, the maximum age of Cuddapah basin is  $<2081.8$  Ma. The minimum age of Papaghni Group is calculated by the age of the mafic igneous rocks in Tadpatri Formation as 1.89–1.88 Ga (e.g., Rb–Sr Whole-rock by Bhaskar Rao *et al.* 1995; <sup>40</sup>Ar–<sup>39</sup>Ar Phlogopite age by Anand *et al.* 2003; U–Pb IDTIMS Baddeleyite age by French *et al.* (2008). Sheppard *et al.* (2017) dated the Tadpatri felsic tuffs at  $1862 \pm 9$  Ma by the zircon U–Pb analysis using the sensitive high-resolution ion microprobe (SHRIMP). Therefore, the age of Tadpatri Formation (excluding the Gandikota Quartzite) can be considered as about 1.86 Ga. The  $1207 \pm 22$  Ma age (U–Pb detrital zircon) of the Gandikota Formation is correlatable with Kurnool Group, which is about 700 Ma younger than the Tadpatri Formation (Collins *et al.* 2015). In this Palaeoproterozoic volcanoclastics of the Tadpatri Formation, there is a significant event of carbonatization, which has been discussed in earlier (Goswami *et al.* 2018; Goswami and Dey 2018). Field evidences suggest younger age of such carbonates as compared to the metastable glassy felsic volcanic rocks. However, in this study the actual time of this carbonatization is calculated as  $\sim 1.2$  Ga by radiometric dating of carbonatized portion (whole rock Pb–Pb).

### 3. Tectonic set-up

The tectonics of this polyhistory basin, which comprises sub-basins, is a matter of considerable debate (Goswami and Upadhyay 2019; Mukherjee

*et al.* 2019). A plausible explanation on the basis of paleostress reconstruction and multiphase weak deformation (Tripathy and Saha 2013; Saha and Tripathy 2015) revealed punctuated evolution of the Cuddapah basin. According to Dasgupta *et al.* (2013) rifting within the Dharwar Craton is possibly related to the igneous emplacement  $\sim 1.9$  Ga during opening of the Cuddapah basin. This age of igneous emplacement is well established by several workers (Chatterjee and Bhattacharji 2001; Anand *et al.* 2003; Halls *et al.* 2007; French *et al.* 2008; Ravikant 2010). This magmatism is described as a part of an 1891–1883 Ma Large Igneous Province (LIP) by French *et al.* (2008) spanning the Dharwar and Bastar cratons.

Saha and Tripathy (2012) opined that the Cuddapah basin is one of the finest examples of intracratonic Proterozoic basins. However, they considered the Nallamalai Fold Belt as a thrust transported unit. According to them the Nallamalai Group is possibly allochthonous and its formation was independent of the Papaghni sub-basin development. Although the transverse faults in the west (viz., Gani-Kalva and Kona faults; see figure 2b) were related to initiation of Papaghni sub-basin, the reactivation of these faults during late contractional deformation is evident from fault-slip analyses (Tripathy 2011; Tripathy and Saha 2013; Saha and Tripathy 2015). This deformation possibly originated from the tectonic juxtaposition of the NFB against the western part of Cuddapah basin during the Late Neoproterozoic (Saha *et al.* 2006).

According to Matin (2015), the Cuddapah basin formed as the frontal part of a larger fold-thrust belt, named the Cuddapah fold-thrust belt. This



belt was possibly formed by amalgamation of Antarctica with the Krishna province of India during the formation of the Rodinia Supercontinent (Matin 2015).

Patranabis-Deb *et al.* (2012) have suggested that the sediments of the Papaghni Group are the product of sea-level rise prior to Columbia assembly (Santosh 2010). Breaking of Columbia and separation of the south Indian craton from the North China craton (cf. Ravikant 2010) is used as an explanation of extension. Breaking up of Rodinia is explained as a possible cause of the formation of Kurnool and Palnad basins.

Based on a comprehensive study on the age distribution of detrital zircons from the different stratigraphic levels, Collins *et al.* (2015) proposed an early phase of marine passive margin basin development by rifting. Mafic magmatism in the Tadpatri Formation is interpreted as plume-related magmatism (Mall *et al.* 2008; Chandrakala *et al.* 2010, 2013). The  $\sim 1.68$ – $1.6$  Ga Krishna orogeny (Henderson *et al.* 2014) plausibly interrupted this plume-modified passive margin environment with westerly supply of sediment from an uplifted eastern block. The Krishna orogeny is related to India–Antarctica collision event during which time the Nallamalai and the Srisailam Group of sediments were deposited (Collins *et al.* 2015). In this way, the earlier passive margin was converted into a foreland basin. After the cessation of sedimentation, a long period of erosion led to denudation of the highlands. Finally, the Gandikota Formation and Kurnool Group were deposited in a fluvial to epicontinental sea environment. However, Gandikota Formation conformably overlies the Tadpatri Formation with gradational contact as can be seen in the cuttings of the Gandikota Gorge nearby the Gandikota fort. Thus, field evidence contradicts the finding of Collins *et al.* (2015).

According to Mukherjee *et al.* (2019), the crescent shape of the Cuddapah basin is mainly due to the thrusting related to the Eastern Ghats Orogeny. This view is mostly corroborated with the explanation on arcuate orogeny/orocline (Tripathy *et al.* 2013). Deformation structures in basement complexes as well as Cuddapah basinal sedimentary rocks indicate at least three tectonic events (Mukherjee *et al.* 2019). These deformation events are responsible for the present basin configuration. The crescent-shape of the Nallamalai fold belt in the east is due to a E–W compression related to thrusting followed by a NNE–SSW

compression (Mukherjee *et al.* 2019). The most common E–W and N–S extension joints in the southern part of the Papaghni sub-basin indicate that the older E–W joints developed by maximum compression ( $\sigma_1$ ) along E–W and minimum compression ( $\sigma_3$ ) along N–S direction (Goswami *et al.* 2012, 2016a). Later N–S joints are related to some modification in the stress field. The conjugate joint sets with NE–SW and N15°W–S15°E trends indicate  $\sim$ N15°E–S15°W acute bisector ( $\sigma_1$ ) direction. Therefore, the maximum compression ( $\sigma_1$ ) direction switched from E–W to NNE–SSW with time and the later stress is mostly responsible for shear fracture and N–S extension fracture development depending upon rheology and orientation of litho-unit (Goswami *et al.* 2012, 2016a).

The Bouguer Gravity anomaly and the DSS profiles were interpreted to describe the Moho boundary at  $\sim 38$ – $40$  km depth below the basin with crustal thinning towards east (Balakrishna 1979; Kaila and Tewari 1985; Reddy *et al.* 2000, 2004; Sarkar *et al.* 2001; Singh *et al.* 2004). DSS studies have also indicated variation in basement depth with different deep-seated faults extending to the mantle and a sediment thickness of  $\sim 8.0$  to  $8.5$  km in the central axial region of the basin (Kaila *et al.* 1979; Kaila and Tewari 1985; Mahadevan 1994). Based on the DSS studies, Tewari and Rao (1987) inferred a high velocity layer at 1.5–6 km depth. This high velocity (6.9 km/sec) layer has also been delineated by Geological Survey of India (GSI) (1981) and in the cross section it corresponds to the base of the Cuddapah sediments (figure 3a, b). The shape of the anomaly connotes a blind lopolith (Chandrakala *et al.* 2010).

#### 4. Geophysical set-up

The structure of the Cuddapah basin and its basement has been interpreted from basic gravity data (Qureshy *et al.* 1968; Kailasam 1976; Venkatakrisnan and Dotiwala 1987; Krishna Brahmam 1989; Verma and Satyanarayana 1990; Ramakrishnan 1991; Ram Babu 1993; Subba Rao 2002), aeromagnetic data (Babu Rao *et al.* 1987; Mishra *et al.* 1987; Babu Rao 1991; Ramakrishnan 1991; Anand and Rajaram 2002; Kishore and Rama Rao 2004) and deep seismic sounding (DSS) profiles (Kaila *et al.* 1979, 1987; Kaila and Tewari 1985; Singh and Mishra 2002; Reddy *et al.* 2004; Chandrakala *et al.* 2013).

The gravity survey data suggested elliptical positive gravity anomaly high with NW–SE elongation below the of Papaghni sub-basin (Balakrishna and Paul 1970; Balakrishna 1979; Mishra *et al.* 1987; Verma and Satyanarayana 1990; Ram Babu 1993). Such positive gravity anomaly has been interpreted in terms of a lower-crustal lensoid mafic body (Grant 1983; Bhattacharji and Singh 1984; Krishna Brahmam 1989). Krishna Brahmam (1989) proposed that a meteorite impact developed the Papaghni sub-basin. On the other hand, Bhattacharji (1987) suggested that the gravity high closures in the Papaghni sub-basin is a manifestation of voluminous mafic intrusion in the upper crust. Grant (1983) invoked presence of a mafic oval-shaped shallow crustal lopoliths in the SW part of the Cuddapah basin.

Aeromagnetic study in the area revealed oval shaped magnetic anomalies with short wavelength (Babu Rao 1991; Kishore and Rama Rao 2004). This indicate that the mafic sills and flows are related to the configuration of the Papaghni sub-basin. Thus, igneous emplacements possibly occur along with the sedimentation at shallow level.

Kaila *et al.* (1979) carried out a detailed deep seismic sounding (DSS) study. The data of Kaila *et al.* (1979) got processed subsequently (Reddy *et al.* 2000, 2004; Chandrakala 2007; Mall *et al.* 2008; Chandrakala *et al.* 2010). Kaila *et al.* (1987) proposed that step faults exist in the basement below the sedimentary rocks of Cuddapah basin. The initial seismic studies reported  $\sim 10$  km thick sediment cover in the Cuddapah basin (Kaila *et al.* 1979; Kaila and Tewari 1985). Later re-examination of data by Chandrakala *et al.* (2013) proposed a sediment thickness of 4 km in the Cuddapah basin. The 12 km thick sediment in the Nallamalai sub-basin is due to tectonic thickening and apparent repetition of beds due to folding and thrusting (Saha 2002; Saha and Chakraborti 2007; Saha *et al.* 2010).

According to Kaila and Tewari (1985), the Cuddapah basin was first created in its western part by down faulting of the crustal block to form the Papaghni sub-basin. Subsequently, the eastern part was down-faulted to form the Nallamalai sub-basin. Further down, faulting towards north created the Srisailam sub-basin. At a later stage, similar faulting gave rise to the Kurnool and the Palnad sub-basins. After the closure of Kurnool sedimentation, the Nallamalai block was uplifted. The low-angle thrust fault on the eastern margin of the Cuddapah basin is suggested to be a

post-Cuddapah phenomenon. Geological sections prepared by the GSI (1981) using the DSS profile data of Kaila *et al.* (1979) also demonstrated mafic lopolith within the Papaghni sub-basin (figure 3a, b) in the SW of the Cuddapah basin. This high-density mafic intrusion in the SW part of the basin is explained as a product of asthenospheric upwelling, which probably developed funnel-shaped bodies in the upper crust (Chatterjee and Bhattacharji 2001). Positive gravity anomaly and DSS profile together showed the Moho at a depth of 38–40 km below the basin with crustal thinning towards east (Balakrishna 1979; Kaila and Tewari 1985; Reddy *et al.* 2000, 2004; Sarkar *et al.* 2001; Singh *et al.* 2004).

## 5. Igneous rock characteristics of the selected study area

A rectangular block of  $\sim 500$  km<sup>2</sup> area is chosen for mapping and detailed outcrop studies of bimodal volcanism, especially felsic volcanic rocks and associated volcanoclastics (figure 4). Petro-mineralogy and geochemical aspects of the mafic volcanics are extensively studied by Chakraborty *et al.* (2016). Five different types of mafic emplacements (*viz.*, (1) differentiated mafic sill, (2) long slender clino-pyroxene bearing doleritic sills, (3) gabbro sills with trachytoid, (4) dolerite sills and (5) fine grained basaltic sills) with different petrographic and geochemical characteristics are identified within the Tadpatri Formation (Chakraborty *et al.* 2016).

In this context, we study the felsic rocks in detail. Occurrences of spherulites, lithophysae and thundereggs are reported from the area and these features are not found in silica-poor rocks. Felsic volcanics are the only host for such features formed by devitrification of metastable glass. Spherulites are identified from typical rounded or spherical aggregates in outcrop and under microscope they show acicular crystals radiating from single point. Lithophysae are also noted as radial or concentric cavities that is hollow, or partly to completely filled with later minerals. According to Winter (2001), the interstitial glass between expanded vesicles become three pointed shards (figure 5a–d) and ductile deformation of highly heated glass leads to bending. We propose this mechanism to form lithophysae. Thundereggs are solid lithophysae lacking radial structure and filled with secondary silica and carbonates (figure 6a, b). Spherulites

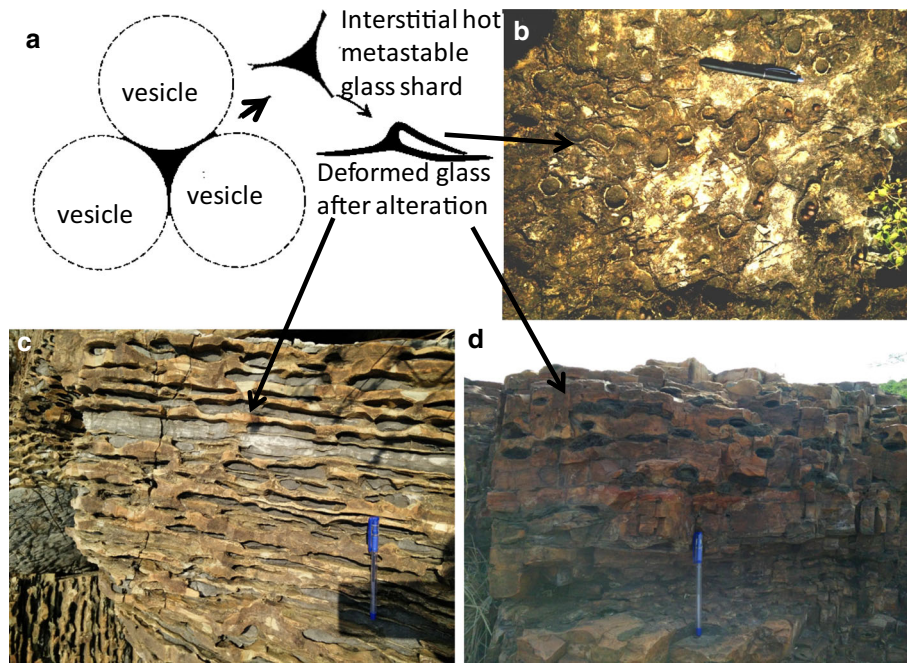


Figure 5. (a) Diagrammatic representation of possible formation mechanism of lithophysae by hot viscous glassy semi-solid materials between gas cavities during ductile flow. (b) Outcrop plan view shows white carbonate minerals replaced partially and occupied spaces between lithophysae, which are formed by volatile escape. (c) Carbonatization in lithophysae chain along meta-stable altered glass. (d) Impure quartz crystals in lithophysae cavity fill.

show diameters of 0.1–2.0 cm formed during devitrification and are associated with lithophysae. Isolated spherulites are generally spherical, but adjacent spherulites often impinge upon one another to produce long chains aligned with flow foliation (figure 7a, b).

Bimodal volcanic association is most remarkable feature in the field (figure 8). In almost all the studied sections, basic volcanics are associated with acid volcanics with concordant relationships. Strike of both the acid and basic flow beds are parallel and no cross-cut relationships exist. Such a bimodal occurrence is typical of a rift basin (Goswami *et al.* 2018; Goswami and Dey 2018).

Under the microscope, radiating arrays of fibrous crystals are identified as spherulites with characteristic dark extinction cross in cross nicol. Some of the incomplete spherulitic growth with radiating crystal fibers results in fan, bow-tie like shapes (figure 9a, b). This is due to parallel arrangements of many radiating fibres to the vibration directions of the polarizer and analyser for any orientation of spherulites. At places well developed flow lines (mostly of 5 mm to 1 cm length) are seen (figure 10). Spherulitic texture indicates cooling and nucleation of material in felsic magma which has achieved supersaturation in the crystal component and spherulitic growth along fractures in volcanic

glass form axiolites formed due to water penetrating along a crack (figure 11). This can promote crystallization of the adjacent glass or viscous melt. Generally, the spherulites are composed of K-feldspar fibres with interstitial quartz. However, spherulitic quartz along with lithic quartz (figure 12a, b) in this Proterozoic terrain is probably due to recrystallization of the original high-temperature SiO<sub>2</sub> polymorphs, which are less stable than quartz at lower temperatures. Flow banding in several tuffaceous units is defined by aligned, coalesced spherulites forming ‘necklace-like’ domains with bulbous margins (figure 12c). The spherulites in tuffaceous rocks consist of fine grained gray to brown clay and quartz. Such spherulites in tuffaceous rocks are highly sericitized formed due to alteration of feldspar (figure 12d, e).

## 6. Sampling and analytical techniques used

Presently the prime focus is given on felsic igneous rocks and only few samples of mafic rocks are studied. For simplicity of understanding, the felsic volcanic and volcanoclastic rocks are discussed separately from the mafic volcanic rocks. Fresh, unaltered samples are difficult to find in this old Proterozoic terrane. However, an effort was made

to collect most fresh samples with less alteration. The geochemical study is used as a supportive tool and interpreted along with field observations and petro-mineralogy. Rock samples were dried after initial cleaning through double distilled water. Then the samples were crushed in jaw crusher to small pieces. The crushed materials were carefully mixed followed by coning and quartering. About

150 g samples were pulverized further in a pulverizer to powder of  $-200$  mesh size.

Twenty eight ( $n = 28$ ) samples including felsic, mafic volcanics and tuffs were collected for detailed geochemical analysis (table 3). The sample locations are shown in the study area map (figure 4). The whole rock chemical analyses of 28 samples were carried out at the Chemistry Laboratories of Atomic Minerals Directorate for Exploration and Research (AMD), Southern Region, Bangalore. The powdered samples were dissolved by acid digestion. In this process 0.5 g of each sample is treated with 5 ml of nitric acid ( $\text{HNO}_3$ ) and 10 ml of hydrofluoric acid (HF) followed by drying. 10 ml of  $\text{HNO}_3$  was further added to the residue. This same procedure was repeated three times for complete removal of HF. Finally, the dried samples were taken up in 100 ml of  $\text{HNO}_3$  ( $\sim 3\%$ ) solution which was used for analysis.

UV-visible spectroscopy (spectrophotometer model no. Analytik Jena Specord 210) was used for determination of  $\text{SiO}_2$  (wt%). Flame photometer (Systronics) was used for analysis of  $\text{Na}_2\text{O}$  and  $\text{K}_2\text{O}$  (Wt%). Inductively Coupled Plasma Optical Emission Spectroscopy (ICPOES) was used for the estimation of  $\text{TiO}_2$ ,  $\text{Al}_2\text{O}_3$ ,  $\text{MgO}$ ,  $\text{MnO}$ ,  $\text{CaO}$ ,  $\text{P}_2\text{O}_5$  (wt%) and Th, Sr, Ba, Nb, Zr, Cr and V (ppm). ICPOES model M/S JobinYvon, France make JY 2000 (2) was used for this study. Atomic Absorption Spectrophotometry (AAS) was used for determination of  $\text{Fe}_2\text{O}_3(\text{total})$  (wt%) and Rb, Cu, Ni and Co (ppm). AAS model GBC-make Savantaa spectrometer was used in this study. Titration was used to determine FeO. Rare Earth Elements (REE) with Y and Sc were also analyzed by ICP-OES after matrix separation. Loss on ignition (LOI) was determined by heating the

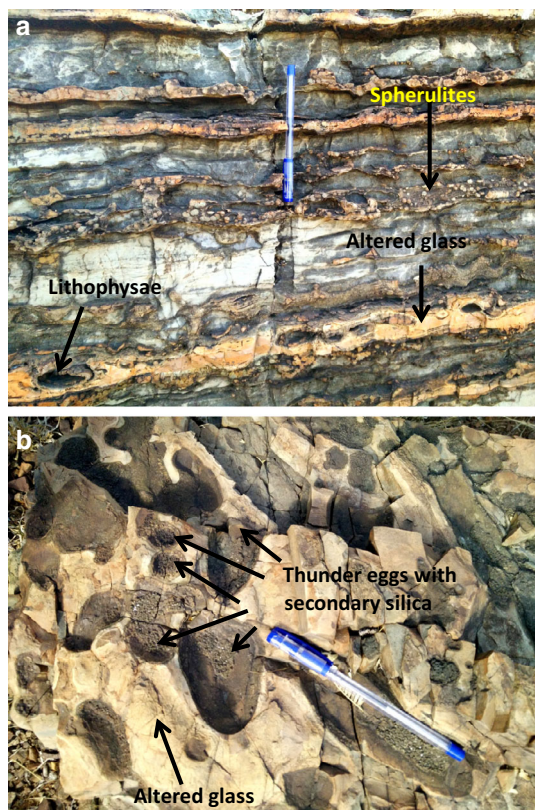


Figure 6. (a) Field outcrop photo of lithophysae, spherulites and glass. (b) Thunder eggs with infilled secondary silica. Both the exposures are located at 1 km SE of Thimmapuram.

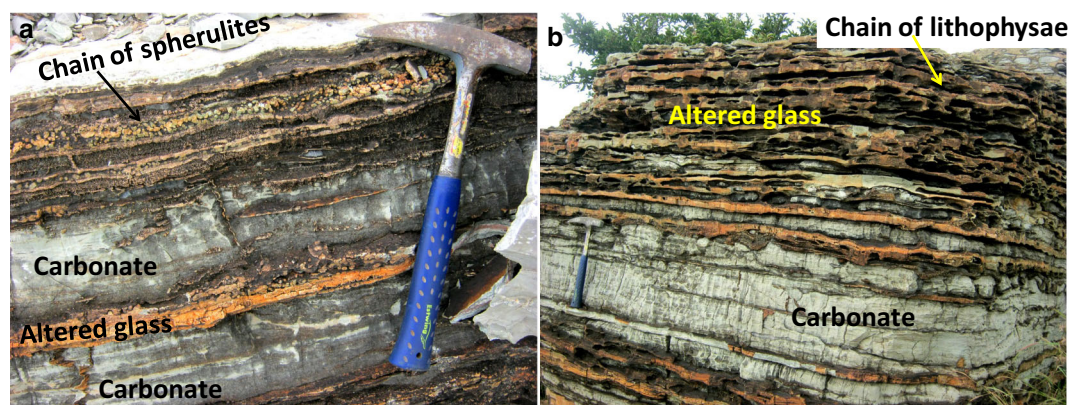


Figure 7. Chain of (a) Spherulites and (b) Lithophysae. The calcite bands were probably formed by later replacement. Both the exposures are located at 1 km SE of Thimmapuram.



Figure 8. Outcrop section of bimodal volcanics showing no crosscutting relationship in between but conformable contacts of flow layers with significant colour and compositional contrast.

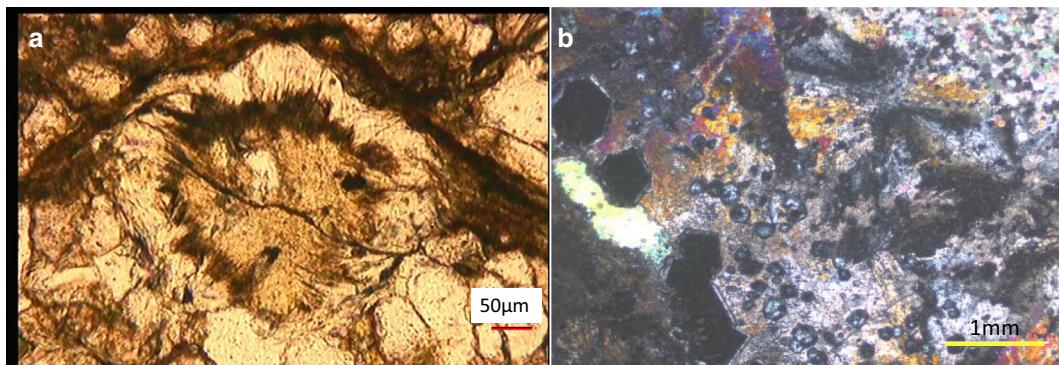


Figure 9. Thin sections of felsic volcanic flow showing radial spherulitic growth. (a) Fan like and (b) bow tie like.

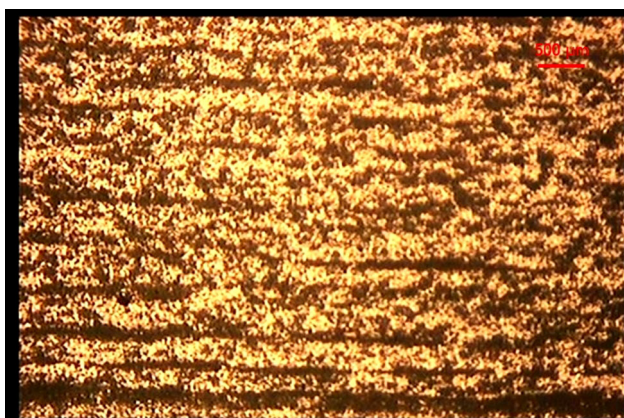


Figure 10. Thin section of flow foliation in glassy rhyolitic flow.

samples at 950°C for about 2 hrs. Geochemical data (tables 4–6) plots suggest wide-ranging composition.

Analytical errors were not same for all the major elements. For SiO<sub>2</sub> analysis error is restricted ( $\pm 1\%$ ). Error for determination of Al<sub>2</sub>O<sub>3</sub>, Fe<sub>2</sub>O<sub>3</sub>, CaO and MgO was also  $\pm 1\%$ . However, TiO<sub>2</sub>,

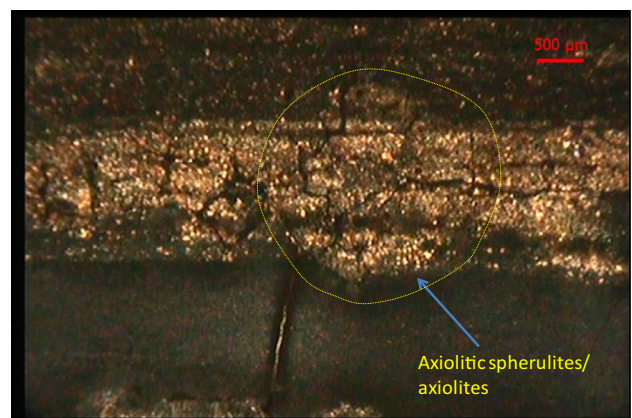


Figure 11. Axiolitic spherulite rich flow banded rhyolite. Transmitted light (TL), crossed nicol (XN).

FeO, MnO, K<sub>2</sub>O and P<sub>2</sub>O<sub>5</sub> data showed errors ranging from  $\pm 2$  to 3%. All other elements showed determination error ranging from  $\pm 5$  to 10%.

The lead isotope systematics of carbonatized portion of felsic volcanics of the study area is undertaken in order to determine the timing as well as extent and nature of carbonatization. The sample

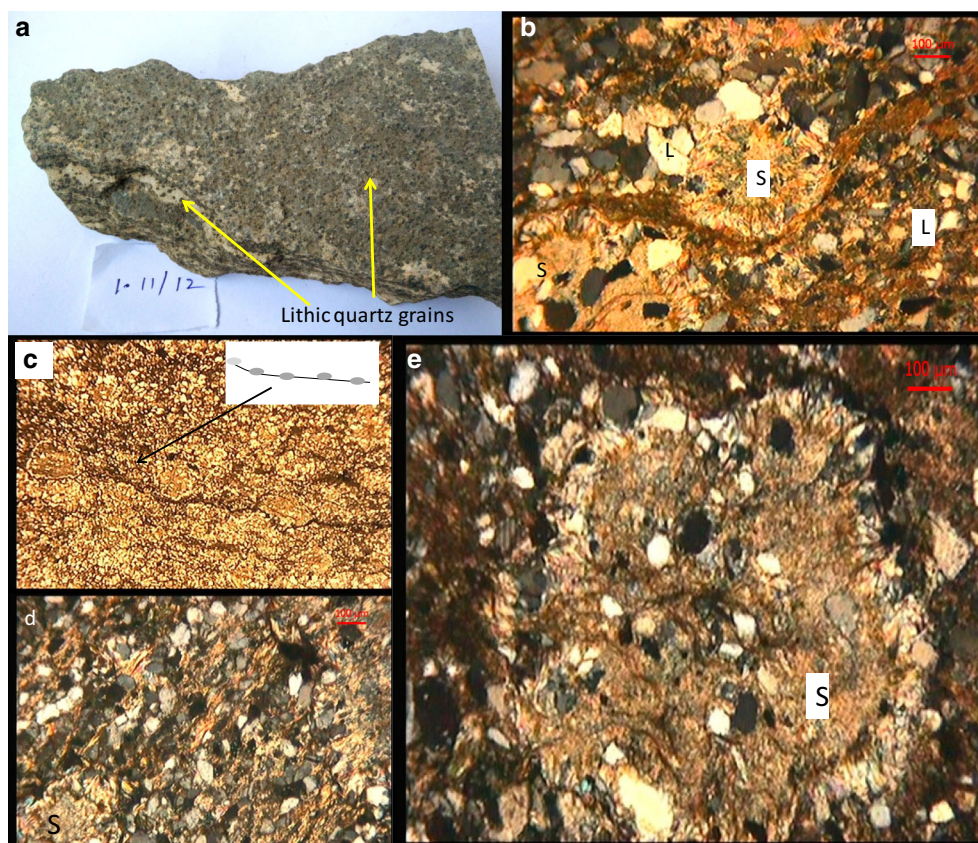


Figure 12. (a) Hand specimen of rhyolitic lithic tuff. (b) Spherulites (S) along with lithic quartz (L). TL, XN. (c) Coalesced spherulites forming necklace-like zones, TL, 1N. (d) Flow banding in lithic rhyolitic tuff, sericitized spherulite (S). TL, XN. (e) Altered spherulites (S) with gray to brown clay and quartz. TL, XN.

(S1) was chosen for step leaching of Pb followed by Pb isotopic study. In fact, five leach fractions were obtained by leaching each sample sequentially with (A) Millipore water, (B) 1M HCl, (C) 2.5M HCl, (D) 4M HCl and, (E) 8M HNO<sub>3</sub>. The residue was separately treated with HF+HNO<sub>3</sub> mixture for its complete digestion. These six fractions were separated for lead (Pb) by AG1X8 ion exchange chromatography. The separated fractions were analyzed on TIMS-Isotopx for the Pb isotopic data at AMD, Hyderabad. Based on the analyses of SRM981 Pb standard, the obtained mass fractionation factor of 0.15% per AMU was applied to correct Pb isotopic ratios. On the basis of the number of duplicate analyses, the  $2\sigma$  analytical error is noted as 0.5% for  $^{206}\text{Pb}/^{204}\text{Pb}$ ,  $^{207}\text{Pb}/^{204}\text{Pb}$  and  $^{208}\text{Pb}/^{204}\text{Pb}$  ratios (table 7). Results of the isotopic standard (SRM983) that was run along with sample, suggest  $^{206}\text{Pb}/^{204}\text{Pb}$  ratio of  $2697.5 \pm 7$ ,  $^{207}\text{Pb}/^{204}\text{Pb}$  ratio of  $191.97 \pm 0.5$  and  $^{208}\text{Pb}/^{204}\text{Pb}$  ratio of  $36.770 \pm 0.09$  ( $n = 10$ ) with total analytical Pb blank of 2 ng. The ratios of  $^{207}\text{Pb}/^{204}\text{Pb}$  and  $^{206}\text{Pb}/^{204}\text{Pb}$  were regressed after the ISOPLOT program of Ludwig (1993), to get isochron age. The Pb–Pb plot of S1 defines an

age of  $1264 \pm 110$  Ma which can be considered as an approximate age of carbonatization.

## 7. Results and interpretation

In the Harker variation diagrams TiO<sub>2</sub>, Al<sub>2</sub>O<sub>3</sub>, MgO and FeOt show decreasing trends with increasing SiO<sub>2</sub> (figure 13). Na<sub>2</sub>O and K<sub>2</sub>O show crude increasing trends with increasing SiO<sub>2</sub>. According to Wilson (1993, 2007), the widespread compositional variation occur due to combined effects of polybaric fractional crystallization, source heterogeneity, crustal contamination and different degrees of partial melting. Despite apparent coherence in trends of multiple plots, conclusion cannot be drawn if there is any genetic line of descent from parent magma by differentiation or fractionation. The total alkali *vs.* silica (TAS) diagram (Le Bas *et al.* 1986) and the R1–R2 plot (De la Roche *et al.* 1980) indicate that the felsic volcanic rocks and tuffs fall dominantly within the rhyolite and dacite fields (figure 14a, b). The rocks are mostly subalkaline in character. The

Table 3. Details of samples analysed geochemically.

Sl. no.	Latitude	Longitude	Rock type	Area	Remarks
1	14.77	78.19	Siltstone tuff	Kondapuram	Grey to red color
2	14.76	78.18	Basalt	Kondapuram	Ophitic texture
3	14.57	78.28	Shale and tuff	Tonduru	Fine ash fall
4	14.61	78.33	Acid volcanic	Mallella	Grey massive
5	14.74	78.27	Acid volcanic	Mangapatnam	Purple color
6	14.71	78.27	Altered volcanic	Mangapatnam	Carbonatization
7	14.69	78.32	Acid volcanics	Denepalle	Lapilli layers
8	14.98	78.01	Lapilli tuff	Sajjaladinne	Lapilli embedded
9	14.98	78.00	Basalt	Sajjaladinne	Plag, px, ophitic
10	15.00	78.01	Tuffaceous silt	Sajjaladinne	Spherulites present
11	14.77	78.12	Acid volcanics	Burzapalle	Lapilli, flow lines
12	14.75	78.17	Lithophysae fill	Thimmapuram	Carbonate rich
13	14.75	78.17	Altered glass	Thimmapuram	Lithophysae rim
14	14.74	78.17	Acid volcanics	Thimmapuram	Secondary silica
15	14.74	78.17	Tuffaceous sand	Thimmapuram	Surge, no cement
16	14.78	78.10	Ash fall tuff	Beduduru	Welded lapilli
17	14.78	78.10	Acid volcanics	Beduduru	Lapilli dots
18	14.77	78.09	Basalt	Beduduru	Lava flow
19	14.78	78.09	Acid volcanics	Beduduru	Greenish grey
20	14.78	78.09	Ash fall tuff	Beduduru	Fine altered ash
21	14.78	78.09	Ash fall tuff	Beduduru	Dots of spherulites
22	14.78	78.09	Acid volcanics	Beduduru	Dots of spherulites
23	14.78	78.09	Acid volcanics	Beduduru	Welded tuff layers
24	14.78	78.09	Acid volcanics	Beduduru	Massive fine
25	14.78	78.09	Acid volcanics	Beduduru	Fine quartz grains
26	14.78	78.09	Acid volcanics	Beduduru	Lapilli, spherulites
27	14.84	78.10	Acid volcanics	Bondladinne	Milky white color
28	14.77	78.10	Lapilli tuff	Ramireddipalle	Purple color

scatter in TAS diagrams is possibly due to the alteration as well as clastic admixing during lava transport. The mafic volcanic rocks plot in the basalt field. In the AFM diagram (Irvine and Baragar 1971), the felsic volcanic rocks and tuffs plot mostly in the calc-alkaline field (figure 15). The mafic volcanic rocks straddle both the tholeiite and calc-alkaline fields. The rocks display peraluminous to metaluminous nature as seen in molar  $\text{Na}_2\text{O}-\text{Al}_2\text{O}_3-\text{K}_2\text{O}$  plot and  $\text{A}/\text{CNK}$  vs.  $\text{A}/\text{NK}$  plot (figure 16a, b) after Shand (1943). The rocks of the study area have undergone different types of post-magmatic alteration (carbonatization, sericitization, chloritization, etc.) and weathering. This limits the usages of major element oxides in characterizing the magma history. Therefore, relatively immobile elements like Ti, Ni, Cr, V, Zr and Nb are taken into consideration of petrogenetic study. Primordial mantle normalized trace element plots indicate enrichment of Large Ion Lithophile Elements (LILE) (Rb, Th and K) and LREE with negative Sr, P and Ti anomalies (figure 17).

Chondrite normalized Rare Earth Elements (REE) patterns are characterized by LREE enrichment, negative Eu anomaly and flat HREE pattern (figure 18). These features, in combination with enrichment of LILE and LREE indicate origin through shallow crustal melting with plagioclase either as a residual or fractionating phase hosting the Eu. This is also supported by the low Sr/Y ratios (ranging from 1 to 10), Sr being hosted by plagioclase in the residue. The mafic volcanic rocks also display LREE enrichment suggesting crustal contamination which can shift the composition of a mantle-derived mafic magma from tholeiitic to calc-alkaline.

The Pb–Pb plot of S1 defines a carbonatization age of  $1264 \pm 110$  Ma (figure 19). This time range represents a significant orogenic event called the Grenville orogeny. According to Chatterjee and Bhattacharji (2001), lineament reactivation in the NW–SE and NE–SW directions was intensified between 1400 and 1200 Ma, leading to the emplacement of several cross cutting dikes in the basin.

Table 4. Major element oxides content (wt%) composition of felsic, mafic volcanic rocks and tuffs from Tadpatri–Tonduru area, Cuddapah district, AP, India.

Sl. no.	Sample no.	SiO <sub>2</sub>	TiO <sub>2</sub>	Al <sub>2</sub> O <sub>3</sub>	Fe <sub>2</sub> O <sub>3</sub>	FeO	MnO	MgO	CaO	Na <sub>2</sub> O	K <sub>2</sub> O	P <sub>2</sub> O <sub>5</sub>	LOI	Total	Mg#	A/CNK
1	S1	75.97	0.10	12.57	0.67	0.10	0.12	0.14	0.71	5.82	1.47	0.01	1.01	98.69	0.26	1.01
2	S2	49.46	1.41	14.14	3.81	11.64	0.20	5.12	6.33	3.29	1.82	0.36	1.75	99.33	0.38	0.75
3	S3	65.50	0.59	13.52	5.56	0.50	0.02	1.20	0.33	0.31	3.00	0.05	7.99	98.57	0.28	3.10
4	S4	69.78	0.12	13.82	0.08	2.51	<0.01	2.92	0.35	3.26	3.88	0.08	1.75	98.55	0.67	1.36
5	S5	76.03	0.08	11.22	1.10	0.65	0.11	0.29	1.74	4.49	2.31	0.01	2.07	100.1	0.24	0.86
6	S6	49.98	1.23	13.95	0.77	8.04	0.09	5.92	5.19	4.80	0.42	0.27	7.92	98.58	0.55	0.78
7	S7	63.55	0.54	16.88	0.80	3.95	<0.01	3.44	0.35	4.28	2.12	0.06	3.04	99.01	0.57	1.69
8	S8	62.51	0.36	15.41	4.24	2.73	<0.01	2.88	0.45	1.99	2.67	0.08	5.54	98.86	0.44	2.21
9	S9	48.95	2.19	12.90	0.85	10.63	0.16	6.99	8.50	2.70	1.50	0.19	3.50	99.06	0.52	0.60
10	S10	56.84	0.48	13.79	1.05	5.32	0.25	2.88	5.08	4.39	1.50	0.06	7.28	98.92	0.45	0.76
11	S11	60.02	0.53	15.40	0.83	5.30	0.08	3.03	1.88	8.54	0.09	0.16	3.17	99.03	0.47	0.88
12	S12	10.06	0.13	2.89	0.74	0.22	0.19	0.98	48.21	1.47	0.02	0.13	33.83	98.87	0.66	0.03
13	S13	46.86	0.50	10.21	1.49	2.37	0.66	5.64	23.25	2.74	0.13	0.13	4.73	98.71	0.73	0.22
14	S14	60.45	0.58	16.61	1.54	1.51	0.08	1.19	3.89	9.49	0.72	0.12	2.25	98.43	0.42	0.71
15	S15	67.82	0.24	15.37	1.66	0.65	<0.01	1.39	0.69	4.45	3.91	0.04	3.11	99.33	0.54	1.20
16	S16	68.55	0.24	14.30	0.13	4.28	<0.01	2.37	0.43	3.91	2.25	0.13	2.46	99.05	0.49	1.48
17	S17	63.43	0.26	15.53	0.18	3.95	0.08	2.48	1.78	4.77	1.95	0.10	4.91	99.42	0.52	1.18
18	S18	47.12	2.22	14.17	2.55	12.60	0.21	5.88	8.34	3.31	0.75	0.35	1.28	98.78	0.41	0.66
19	S19	54.18	0.5	20.33	1.43	7.11	0.04	3.2	0.28	1.76	3.35	0.11	6.31	98.6	0.40	2.89
20	S20	59.96	0.61	18.02	1.44	5.32	<0.01	2.06	0.25	0.77	3.88	0.09	6.13	98.53	0.36	3.04
21	S21	59.63	0.52	19.16	3.63	3.52	<0.01	1.98	0.39	1.42	3.64	0.10	4.68	98.67	0.34	2.74
22	S22	55.04	0.76	19.83	5.88	2.51	<0.01	2.58	0.27	2.02	4.65	0.10	6.1	99.74	0.37	2.24
23	S23	58.46	0.08	15.9	2.63	4.10	0.23	2.81	3.33	6.02	0.55	0.12	4.95	99.18	0.44	0.96
24	S24	6.48	0.07	2.44	1.12	0.93	0.23	0.9	47.97	0.56	0.16	0.04	37.82	98.72	0.45	0.03
25	S25	63.88	0.07	8.1	2.31	9.27	0.27	3.27	3.92	1.03	0.06	0.06	6.82	99.06	0.34	0.91
26	S26	65.82	0.2	14.76	3.87	2.66	0.23	1.71	0.23	5.09	0.85	0.15	2.96	98.53	0.33	1.52
27	S27	71.43	0.34	13.95	0.45	1.51	0.34	0.87	0.34	3.3	5.11	0.07	1.69	99.4	0.45	1.21
28	S28	56.55	0.59	20.44	6.72	1.37	0.32	2.17	0.46	0.64	4.04	0.09	5.23	98.62	0.34	3.26

## 8. Discussions

Volcanoes generally consist of volcanic edifice, plumbing system and deeper magma reservoir. The present study attempts to understand the surface and, to some extent, the subsurface processes associated with the Tadpatri volcanism. The deeper system can be accessible in the eroded portions of active volcanoes or, in extinct eroded volcanoes like the present case of the Proterozoic Tadpatri Formation. The aim is to interpret the shallower and deeper phenomenon of past volcanoes so that the relationships between the magma generation and the nature of country rock can be understood.

The oval-shaped gravity high over the Papaghnri sub-basin has been commonly interpreted in terms of lopolithic intrusions (Grant 1983; Bhattacharji and Singh 1984; Chatterjee and Bhattacharji 2001). These igneous intrusions were possibly related to rifting within the Dharwar craton at

around 1.9 Ga and formation of the Cuddapah basin (Chatterjee and Bhattacharji 2001; Anand *et al.* 2003; Halls *et al.* 2007; French *et al.* 2008; Ravikant 2010). The coeval felsic volcanic rocks of the Tadpatri Formation were probably linked with the spatially associated mafic volcanic and intrusive rocks. These mafic and felsic volcanic rocks show concordant relationship, which also suggest a possible link between them.

### 8.1 Tectonics

The felsic volcanic and volcanoclastic rocks of the Tadpatri Formation display enrichment in LREEs and LILE such as Rb, Ba and K (figures 17 and 18). The fractionated LREE, negative Eu anomaly and flat HREE patterns (figure 18) as well as low Sr/Y ratios indicate shallow melting of a crustal source (Goswami 2019). In the normal condition, the geothermal gradient is not high enough to melt



Table 5. Trace element (ppm) composition of felsic, mafic volcanic rocks and tuffs from Tadpatri–Tonduru area, Cuddapah district, AP, India.

Sl. no.	Sample no.	Ba	Cu	Co	Ni	Rb	V	Cr	Sr	Th	Zr	Nb	Rb/Sr
1	S1	314	18	10	<10	54	10	18	60	18	137	355	0.90
2	S2	672	53	49	37	44	186	32	217	<10	137	<10	0.20
3	S3	380	14	16	44	136	70	92	52	18	158	<10	2.62
4	S4	448	<10	<10	<10	132	20	38	42	32	402	<10	3.14
5	S5	520	<10	<10	<10	80	10	30	79	12	110	<10	1.01
6	S6	82	95	43	44	18	190	64	36	<10	128	<10	0.50
7	S7	280	<10	12	32	48	56	86	29	25	184	75	1.66
8	S8	330	<10	16	37	42	62	80	47	18	147	53	0.89
9	S9	380	145	52	150	32	214	190	166	<10	158	<10	0.19
10	S10	282	205	15	25	<10	53	74	65	18	127	<10	–
11	S11	90	197	14	30	<10	71	85	36	27	181	<10	–
12	S12	66	10	<10	<10	<10	<10	<10	60	10	64	<10	–
13	S13	38	387	<10	18	<10	40	58	54	18	108	<10	–
14	S14	130	20	<10	10	124	58	76	26	18	127	<10	4.77
15	S15	534	<10	<10	243	86	22	40	64	34	545	<10	1.34
16	S16	294	152	15	30	102	34	53	53	23	182	<10	1.92
17	S17	164	<10	13	54	<10	64	65	37	15	200	<10	–
18	S18	244	183	50	60	166	20	146	210	<10	190	<10	0.79
19	S19	300	130	17	42	170	78	110	15	17	176	35	11.33
20	S20	385	<10	10	47	200	85	98	24	15	170	12	8.33
21	S21	387	<10	13	40	192	92	106	24	15	172	<10	8.00
22	S22	480	<10	10	40	218	112	98	22	15	176	28	9.91
23	S23	124	106	14	33	26	62	80	97	40	398	<10	0.27
24	S24	78	24	<10	<10	<10	<10	10	82	12	42	<10	–
25	S25	78	82	18	30	<10	34	78	17	<10	90	<10	–
26	S26	234	28	12	20	52	42	54	74	20	242	12	0.70
27	S27	725	40	<10	<10	162	20	34	74	28	282	<10	2.19
28	S28	45	<10	10	47	198	92	100	30	30	156	12	6.60

rocks within the continental crust (Alfe *et al.* 2003). Therefore, an external heat source is required to generate magma through melting of the continental crust. Th/Yb ratio compared to primitive mantle or mantle array is higher and thus the geochemical signatures suggest a rift set-up for the Papaghni sub-basin. The reactivation of pre-existing faults is indicated from paleomagnetic studies (Balakrishna *et al.* 1972; Kumar and Bhalla 1983; Hargraves and Bhalla 1983).

The mafic sills within the Tadpatri Formation yielded a U–Pb IDTIMS baddeleyite age of  $1885 \pm 3.1$  Ma (French *et al.* 2008) and an Ar–Ar phlogopite age of  $1899 \pm 20$  (Anand *et al.* 2003). Recently, Sheppard *et al.* (2017) reported a U–Pb (SHRIMP) zircon age of  $1862 \pm 9$  Ma from a felsic volcanic rock of the Tadpatri Formation. These ages suggest contemporaneity between the mafic and felsic intrusive and volcanic rocks of the Tadpatri Formation.

Regional geological set-up, rock association, intrabasinal igneous activity, geochronology, deep basinal architecture and geophysical studies suggested a rift-related origin for the Cuddapah basin (Nagaraja Rao *et al.* 1987; Anand *et al.* 2003; Manikyamba *et al.* 2008; Patranabis-Deb *et al.* 2012; Chandrakala *et al.* 2013; Chakraborty *et al.* 2016; Sheppard *et al.* 2017). Nagaraja Rao *et al.* (1987) proposed existence of lopolith within the southwestern part of the Cuddapah basin based on harmonic inversion of the gravity and magnetic data of Mishra *et al.* (1985). Gravity high in the Papaghni sub-basin is situated almost concentrically with circular central gravity low (Balakrishna 1979; Grant 1983; Bhattacharji 1987; Ram Babu 1993; Singh and Mishra 2002). The broadly oval-shaped, the gravity high was ascribed to shallow crustal lopolithic intrusion by Grant (1983) as well.

Mall *et al.* (2008) prepared a 2-D geophysical model for the crustal structures below the Cuddapah

Table 6. REEs, Y and Sc (ppm) content of felsic, mafic volcanic rocks and tuffs from Tadpatri–Tonduru area, Cuddapah district, AP, India.

Sl. no.	Sample no.	La	Ce	Pr	Nd	Sm	Eu	Gd	Tb	Dy	Ho	Er	Tm	Yb	Lu	Y	Sc	Sr/Y
1	S1	16	32	<5	20	<5	<0.5	2	<2	3	<2	<2	<2	1.0	<0.5	14	4	4.3
2	S2	26	38	6	22	6	0.8	3	<2	4	<2	4	<2	2.0	<0.5	20	20	10.9
3	S3	57	98	11	44	8	0.8	4	<2	4	<2	3	<2	2.0	<0.5	20	14	2.6
4	S4	44	67	8	30	6.0	<0.5	3	<2	3	<2	2	<2	2.0	<0.5	20	5	2.1
5	S5	8	12	<5	6	<5	<0.5	<2	<2	2	<2	<2	<2	1.0	<0.5	10	3	7.9
6	S6	25	40	5	18	<5	0.6	4	<2	5	<2	3	<2	3.0	<0.5	26	30	1.4
7	S7	52	82	8	37	7	0.8	4	<2	4	<2	2	<2	2.0	<0.5	20	12	1.5
8	S8	37	60	8	30	6	<0.5	3	<2	3	<2	2	<2	2.0	<0.5	18	12	2.6
9	S9	15	27	<5	20	<5	1.2	5	<2	5	<2	3	<2	2.0	<0.5	26	24	6.4
10	S10	47	70	8	34	7.0	1.4	6	<2	5	<2	3	<2	2.0	<0.5	32	11	2.0
11	S11	79	128	18	65	13	1.6	9	<2	6	<2	3	<2	3.0	<0.5	32	14	1.1
12	S12	16	24	<5	12	<5	<0.5	<2	<2	<2	<2	<2	<2	<1	<0.5	12	2	5.0
13	S13	44	70	7	26	5.0	<0.5	2	<2	2	<2	<2	<2	1.0	<0.5	14	11	3.9
14	S14	49	89	10	36	7.0	<0.5	5	<2	5	<2	3	<2	2.0	<0.5	28	13	0.9
15	S15	48	81	7	35	6	1.2	3	<2	2	<2	<2	<2	1.0	<0.5	14	3	4.6
16	S16	39	67	6	32	6.0	0.9	3	<2	3	<2	2	<2	1.0	<0.5	18	6	2.9
17	S17	50	86	9	41	8	1.5	5	<2	5	<2	3	<2	2.0	0.6	30	11	1.2
18	S18	20	40	4	30	6.0	1.8	6	<2	6	<2	4	<2	3.0	0.6	32	25	6.6
19	S19	47	81	8	37	7	1.1	4	<2	4	<2	3	<2	2	0.5	20	15	0.8
20	S20	47	78	8	40	7	1.3	4	<2	5	<2	3	<2	2	0.5	25	15	1.0
21	S21	45	75	9	40	5	1.2	3	<2	4	<2	2	<2	2	0.5	20	17	1.2
22	S22	42	85	9	41	7	1.3	4	<2	4	<2	3	<2	3	0.6	23	20	1.0
23	S23	32	72	7	30	6	1.6	5	<2	4	<2	3	<2	2	0.6	25	11	3.9
24	S24	8	13	<5	7	<5	<0.5	<2	<2	<2	<2	<2	<2	<1	<0.5	9	2	9.1
25	S25	25	46	<5	21	<5	0.7	2	<2	3	<2	<2	<2	1	<0.5	18	6	0.9
26	S26	31	69	<5	28	6	1.1	4	<2	5	<2	3	<2	3	0.6	24	8	3.1
27	S27	23	35	<5	15	<5	0.5	<2	<2	<2	<2	<2	<2	1	<0.5	10	2	7.4
28	S28	46	77	8	38	7	1.4	4	<2	4	<2	3	<2	2	0.5	25	16	1.2

Table 7. Pb–Pb data of carbonatized sample from the study area.

Sample no.	$^{206}\text{Pb}/^{204}\text{Pb}$	$^{207}\text{Pb}/^{204}\text{Pb}$	$^{208}\text{Pb}/^{204}\text{Pb}$
S1 (A)	95.618	22.337	39.229
S1 (B)	45.995	19.429	68.591
S1 (C)	52.249	19.737	64.618
S1 (D)	1534.4	142.17	56.530
S1 (E)	68.981	20.464	54.035
S1 (Res)	27.675	17.027	42.180
Errors (%)	0.5	0.5	0.5

basin. They have noted deep-seated thermal anomaly attributed to a mantle plume. Based on seismic data interpretation, Chandrakala *et al.* (2010) have also proposed a mantle plume in the same area. Deep seismic studies (Kaila *et al.* 1979, 1987; Reddy *et al.* 2000, 2004; Sarkar *et al.* 2001; Chandrakala *et al.* 2013) revealed presence of N–S and NW–SE faults

within the Papaghni sub-basin, which extend up to the Moho. Moreover, mantle plume is considered as a triggering cause the formation of the Cuddapah basin development by some authors (Mall *et al.* 2008; Chandrakala *et al.* 2010).

Anand *et al.* (2003) described the Proterozoic melt generation processes beneath the southwestern part of the Cuddapah basin on the basis of petrography, whole-rock and mineral geochemistry of mafic igneous rocks. They have concluded that lithospheric stretching and mantle melting was associated with intra-cratonic passive rifting. However, there are distinct signatures of active rifting in the Papaghni sub-basin which has been substantiated in this study.

Barberi *et al.* (1982) classified rifts into low and high volcanicity rifts on the basis of relative volume of volcanic eruption materials. Low volcanicity rifts (LVR) show low volume of volcanic products, low crustal extension rates,

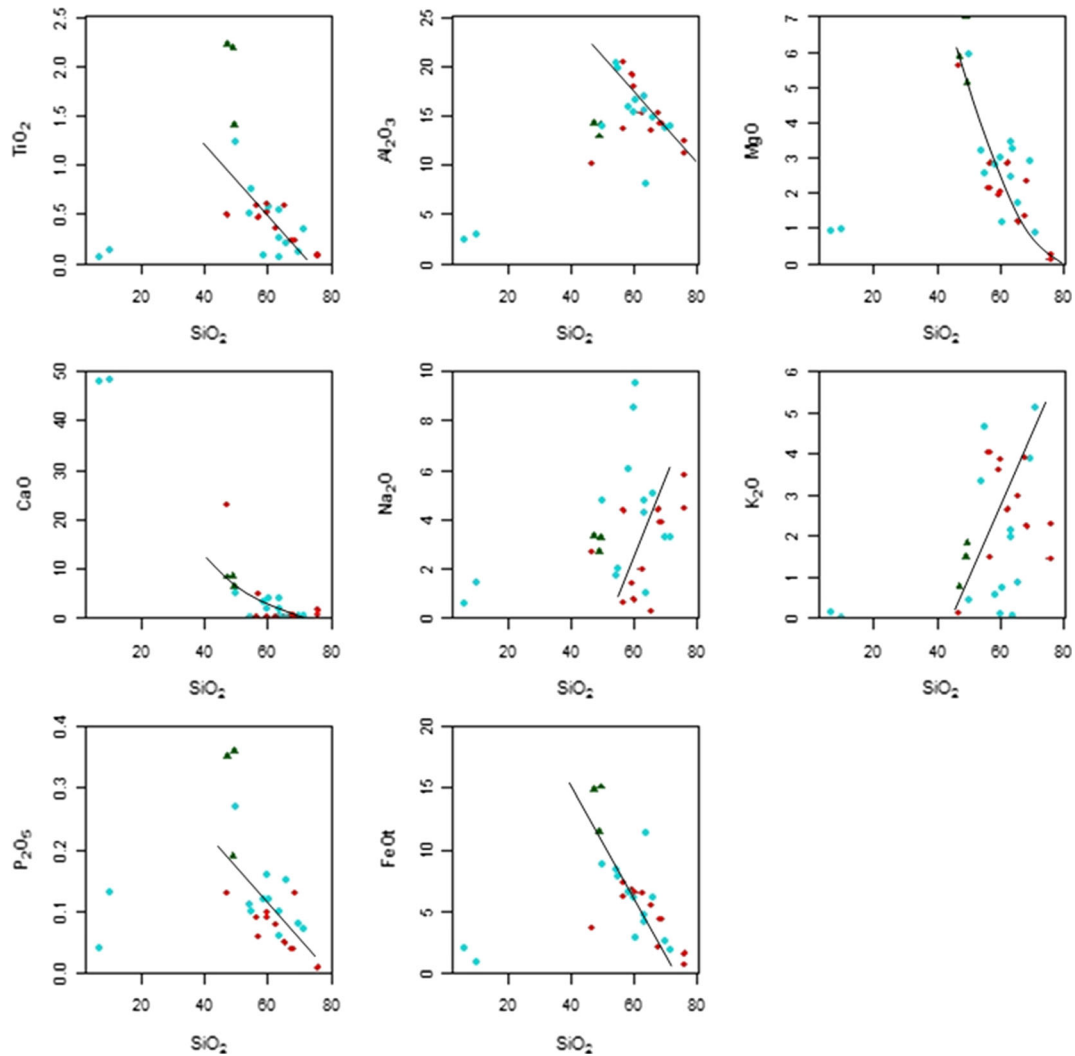


Figure 13. Variation of major oxides against  $\text{SiO}_2$  (all in wt%). Cyan dots are felsic volcanic rocks, red dots are tuff and green triangles are mafic volcanic rocks.

discontinuous volcanism and a variety of basaltic magma composition with smaller quantity of felsic eruption. The lesser volume of volcanic products compared to sediments in the Papaghni sub-basin is possibly due to lower rate of crustal extension. There were discontinuous volcanism throughout the basin. The variation in basaltic magma composition (Chakraborty *et al.* 2016) and relatively small volumes of felsic volcanic rocks within the Tadpatri Formation are significant. These facts indicate that the magmatism in the study area can be related to LVR (Barberi *et al.* 1982).

Chakraborty *et al.* (2016) recognized five varieties of mafic intrusives in the Papaghni sub-basin on the basis of petrographic and geochemical characteristics. The mafic rocks were interpreted as the product of partial melting of a metasomatized subcrustal lithospheric mantle in varying degrees. Chakraborty *et al.* (2016) also interpreted

the mineral chemistry and rock chemistry of mafic sills and lava to have alkaline affinity and suggested a riftogenic set-up for the mafic volcanic rocks. It is notable that alkaline volcanism is a characteristic feature of continental rift setting (Fitton and Upton 1987; Winter 2001; Ranjith *et al.* 2016) which also support our view.

The geodynamic reason of Cuddapah rifting is controversial (Anand *et al.* 2003; French *et al.* 2008; Mall *et al.* 2008; Chandrakala *et al.* 2010; Ravikant 2010; Saha and Tripathy 2012; Patranabis-Deb *et al.* 2012; Collins *et al.* 2015; Chakraborty *et al.* 2016; Sheppard *et al.* 2017; Mukherjee *et al.* 2019). A popular model for the  $\sim 1.9$  Ga rifting, formation of the Cuddapah basin and associated mafic intrusive and volcanic activity envisages mantle upwelling below the eastern part of the Dharwar craton (Chatterjee and Bhattacharji 2001; Mall *et al.* 2008; Chandrakala *et al.*

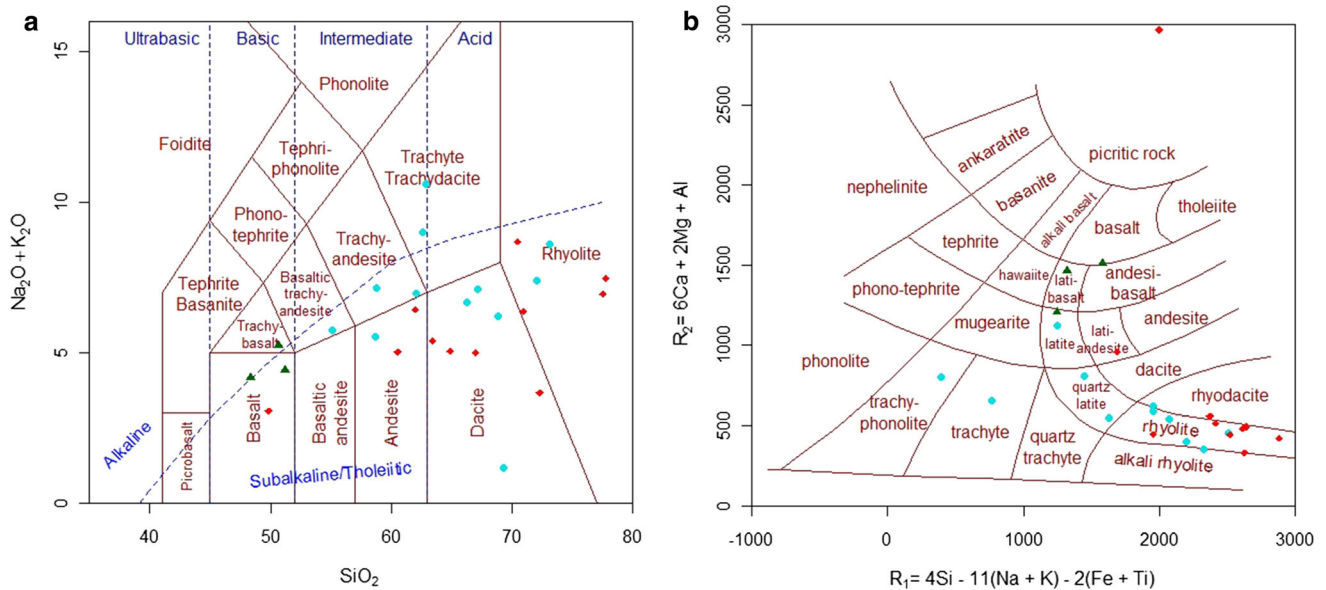


Figure 14. (a) TAS diagram plot, as proposed by Le Bas *et al.* (1986). (b) R1–R2 plot (after De la Roche *et al.* 1980). Cyan dots are felsic volcanic rocks, red dots are tuff and green triangles are mafic volcanic rocks.

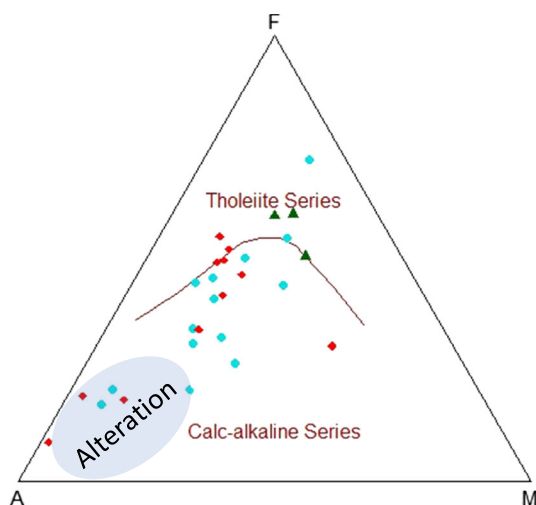


Figure 15.  $\text{Al}_2\text{O}_3$ – $\text{FeO}$ – $\text{MgO}$  (AFM) plot (after Irvine and Barager 1971) of the samples indicating tholeiitic nature of magma.

2010; Collins *et al.* 2015; Chakraborty *et al.* 2016). This model invokes rise of hot asthenospheric material and attendant stretching and thinning of overlying lithosphere. This resulted in continental rifting and formation of the intracratonic/pericratonic basin.

The mafic magma was possibly generated by decompression melting of the upwelling mantle (White and McKenzie 1989; Keen *et al.* 1994; Mall *et al.* 2008; Chandrakala *et al.* 2010, 2013; Rychert *et al.* 2012; Wright *et al.* 2016; Chakraborty *et al.* 2016). Underplating and intraplating of this mafic magma supplied heat into the continental crust which probably caused increased geothermal

gradient and intracrustal melting. In figure 20(a), a scenario of the partial melting of rocks with elevated geothermal gradient is schematically represented. The elevated geothermal gradient can cross the solidus inducing partial melting of the continental crust. This mechanism is being proposed as the origin of felsic volcanism within the Tadpatri Formation (figure 20b).

The origin of rift basin is related to thinning of the lithosphere (e.g., Dasgupta and Mukherjee 2017). The cause of lithospheric extension and thinning is explained differently (Neumann and Ramberg 1978; Illies 1981; Palmason 1982; Morgan and Baker 1983; Neugebauer 1983; Keen 1985; Dewey and Hancock 1987; Khain 1992; Ziegler 1992; Thompson and Gibson 1994; Ruppel 1995; Brun 1999; Corti 2009). Generally, continental rifts are fault-bounded basins produced by extension of continental crust (Dietz 1963; Dewey and Bird 1970; Falvey 1974; Kinsman 1975; Veevers 1981). With increasing amount of stretching, arrays of normal fault may develop. These faults control subsidence and heat flow within rift-related basins formed over thinned continental crust (Withjack *et al.* 2002).

Broadly, the thinning of lithosphere can be related to two different mechanisms (Sengör and Burke 1978). First, it may result from the ascent of a mantle plume (figure 21a). Second, extensional stress can stretch the crust and the lithospheric mantle (figure 21b). Sengör and Burke (1978) described these two mechanisms as active and

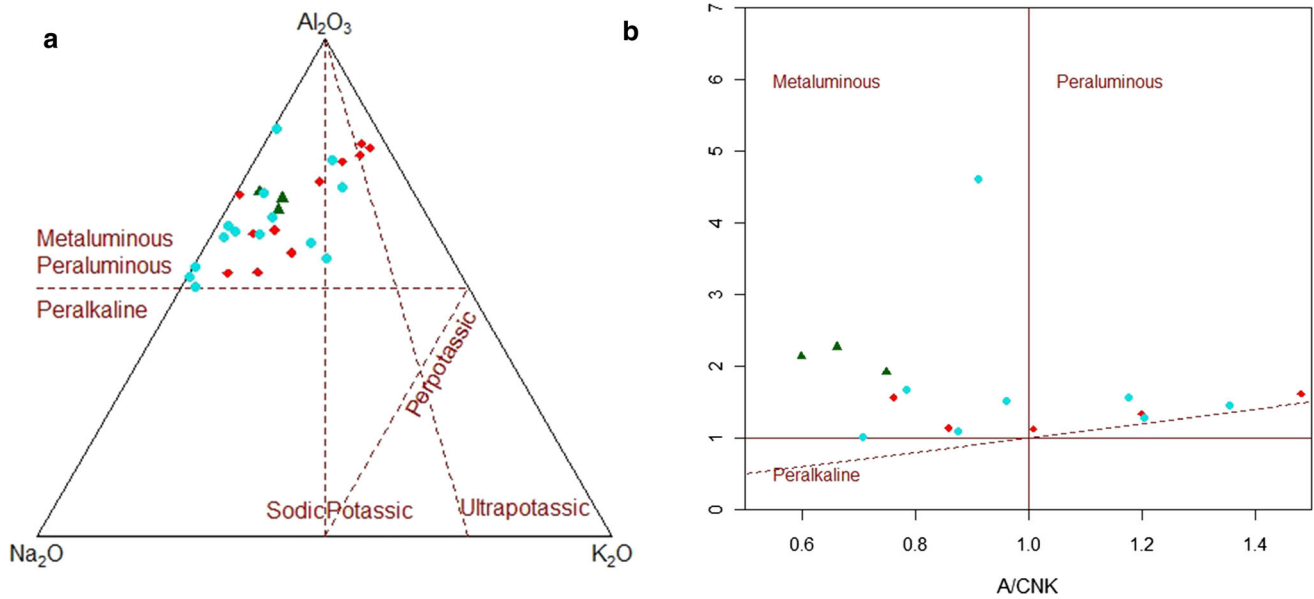


Figure 16. (a) The metaluminous to peraluminous nature of rocks shown by triangular  $Al_2O_3$ – $K_2O$ – $Na_2O$  diagram. (b) A/CNK vs. A/NK plot after Shand (1943) also suggest metaluminous to peraluminous type.

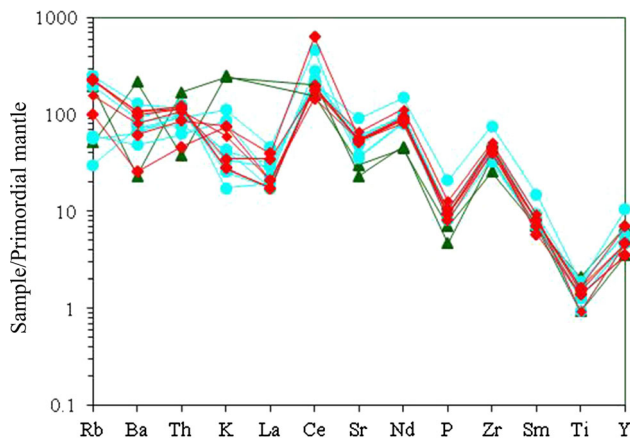


Figure 17. Primordial mantle (Wood *et al.* 1979) normalized multi-elemental diagram for tuff, mafic and felsic volcanic rocks from Tadpatri Formation. Selected samples with relatively more complete range of quantified elemental values are plotted.

passive rifting, respectively. A combination of ‘active’ and ‘passive’ processes may also operate (Marle 2011).

The typical elevated rift flank topography is characteristic feature of mostly active rifts (Bhattacharya and Chakraborty 2000; Allen and Allen 2005; Zhiyuan Ge *et al.* 2016). This elevated rift flank topography bordering the basin may also be regarded as ‘Rift shoulder’ (Bhattacharya and Chakraborty 2000; Goswami *et al.* 2016a; Bhattacharjee *et al.* 2018; Mukherjee *et al.* 2019) (figure 21c). Withjack *et al.* (2002) explained the developments of rift shoulders in terms of footwall upliftment of the basin margin fault. According to

Chaudhuri *et al.* (2002), the basin-margin faults in Cuddapah basin controlled the broad geometry and evolution of the basins. Based on the fault controlled differential subsidence and uplifts and syn-sedimentary events with limited volcanism the Cuddapah basin was interpreted as fossil rift (Chaudhuri *et al.* 2002).

In case of passive rifting sedimentation occurs in depressed graben without igneous activity (figure 21d) (Marle 2011). However, this is not the case in Cuddapah basin. Geological as well as geophysical observations in active rift areas have suggested presence of active volcanoes and elevated heat flows, high seismicity, thinner crust with elevated Moho beneath the rift zones (Morgan and Baker 1983; Lysak 1987; Wheildon *et al.* 1994; Hochstein 2005; Kandie 2015). Previous discussions suggest that bimodal magmatism in the Tadpatri Formation is contemporaneous with sedimentation as revealed by field, structural, geophysical and geochronological data (see sections 2–5, 7). Such coeval sedimentation and magmatism is common in active rifting. Therefore, active rifting for the development of the Cuddapah basin can be inferred from the present state of knowledge. This study envisages that active rifting and associated lopolithic emplacement is related to basin development. Rift basins usually show normal dip slip faults and variable number of strike slip faults (Withjack *et al.* 2002; Pluijm and Marshak 2004). Depending on the rift axis orientation in relation to the extension direction, normal fault

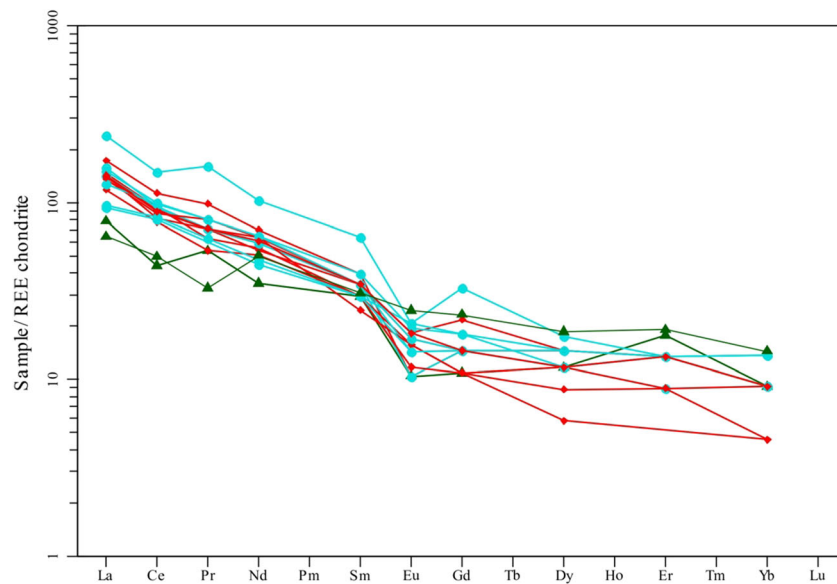


Figure 18. Chondrite (Boynton 1984) normalized REE diagram of tuff, mafic and felsic volcanic rocks from Tadpatri Formation. Selected samples with relatively more complete range of quantified REE values are plotted.

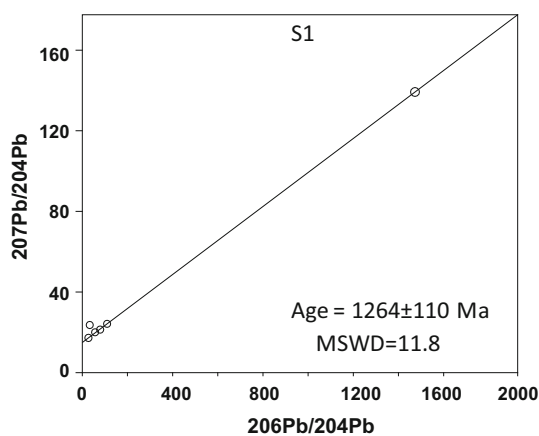


Figure 19. Pb–Pb age data plot of sample S1 shows  $\sim 1264$  Ma age of carbonatization.

arrays with synthetic and antithetic fashion develop. We suggest that the Papaghni sub-basin development was associated with shallow crustal lopolithic intrusion with a system of thin feeder channels. The area (figure 22a) was possibly affected by asthenospheric upwelling and lithospheric stretching (figure 22b) during Late Palaeoproterozoic. The stretching presumably developed listric normal faults commonly associated with rift basins (Bally *et al.* 1981; Shelton 1984; Allen and Allen 2005). These listric faults are concave upward, i.e., flatten with depth (figure 22c). It is envisioned that the subsidiary normal faults may be dipping either in the same direction (synthetic faults) or in the opposite direction (antithetic faults) (Withjack *et al.* 2002;

Pluijm and Marshak 2004). Therefore, the initially developed basin was bounded by normal faults dipping towards each other (figure 22d). These faults might have been merged at depth with possible flat decollement or truncated by detachment fault that develops during extension (Pluijm and Marshak 2004). The curved, downward flattening listric faults are possibly associated with rotation of hanging-wall blocks (Davis and Reynolds 1996) (figure 22d). Downward movement on concave up listric normal faults rotate the hanging-wall blocks, so that the blocks progressively tilt during regional extension (Davis and Reynolds 1996; Davis *et al.* 2012). The amount of tilting is proportional to the amount of displacement on the fault. Because of the curvature of listric faults, movement of the hanging-wall block along a subhorizontal detachment may create a gap (Wernicke and Burchfiel 1982; Gibbs 1983) (figure 22e). The tilting of hangwall driven by gravity to adjust the gap may lead to the development of roll-over antiform (Wernicke and Burchfiel 1982; Gibbs 1983, 1984; Krezsek *et al.* 2007). The weak fault planes possibly provided the pathways for emplacement and eruption of mantle-derived mafic magma. These are fissure-type eruptions bounded by listric faults which produced the probable lopolithic geometry (figure 22f). The emplacement of mafic magma possibly supplied heat within the crust. It is contemplated that the attendant crustal melting generated the felsic volcanic and the associated volcanoclastic rocks of the Tadpatri Formation (figure 22f).

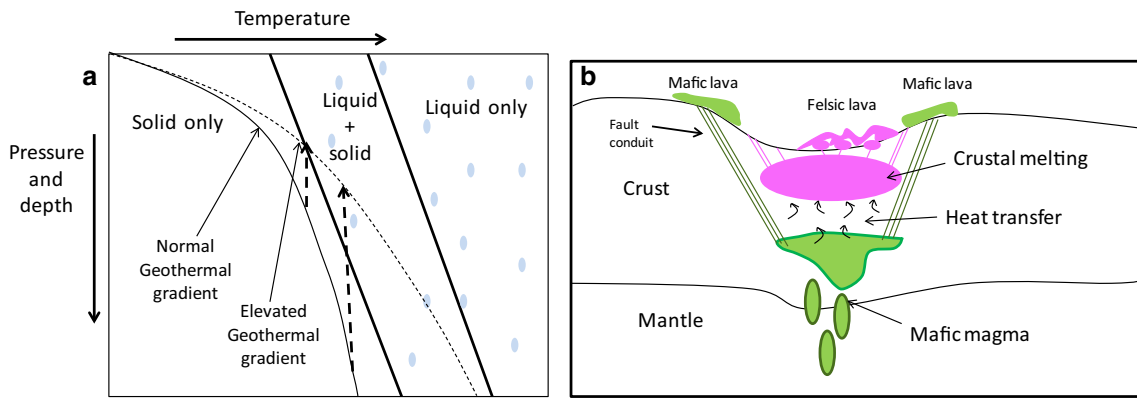


Figure 20. Schematic representation of possible condition for the genesis of Tadpatri igneous rocks. (a) Pressure (P) vs. temperature (T) diagram showing probable condition of elevated geothermal gradient in the case of mantle upwelling and melting. (b) Model showing the possible explanation of bimodal volcanism in the Tadpatri Formation. Emplacement of mantle derived mafic magma triggered crustal melting and generation of felsic magma.

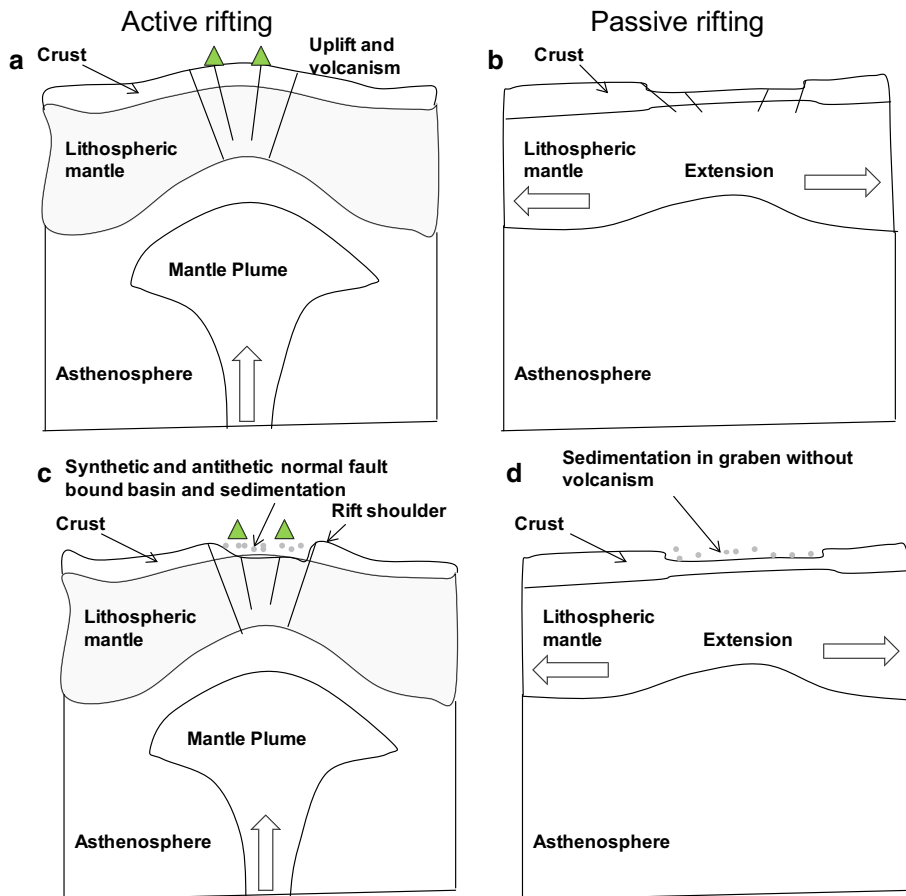


Figure 21. Conceptual model showing tectonic evolution for ‘Active’ and ‘Passive’ rifting. (a) Initial phase of active rifting with plume associated crustal thinning. (b) Initiation of passive rifting associated with remote extension stress and stretching of lithosphere. (c) Later stage of active rifting. The basin development with typical rift shoulder margin and volcano-sedimentary basin fill. (d) Later stage of passive rifting without volcanism. Only sedimentary rocks occur in the basin. Rift shoulder is not commonly developed in passive rifting.

### 8.2 Basin evolution model

The 3 Ga supercontinent termed ‘Ur’ after Rogers (1993) can be regarded as an initial stable crust. By the Late Palaeoproterozoic, the crustal thickness

became sufficient to resist direct mantle outpouring to the surface. Hence the mantle underplating lead to stretching and thinning of the crust and thus initiation of rifting. The presence of 2.3–2.1 Ga dyke swarms (French and Heaman 2010; Belica

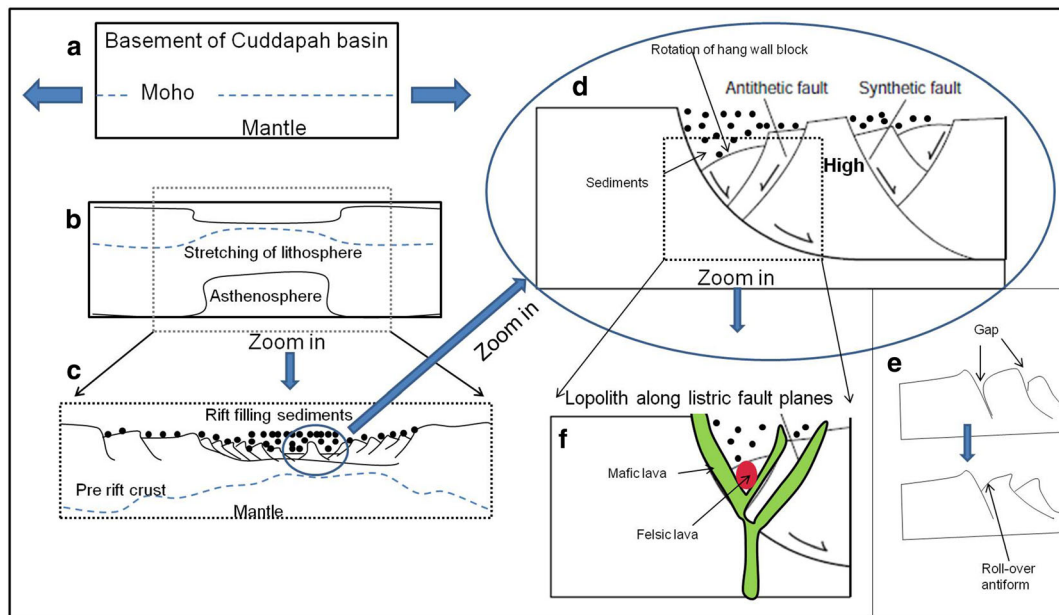


Figure 22. Model suggesting basin evolution during the initial stage of Cuddapah basin formation. (a) Initial undisturbed basement and Moho. (b) Asthenospheric upwelling related to plume and domal upliftment of Moho. (c) Lithospheric stretching lead to development of series of listric normal faults of synthetic and antithetic types and sedimentation in the basin. (d) Zoomed in view of the part of the rift system. (e) Creation of gap due to stretching of lithosphere and development of roll over antiform. (f) Rifting and emplacement of mantle-derived mafic magma along the listric fault planes. Such geometry of igneous bodies along curve fault planes can be regarded as lopoliths. Generation of felsic magma due to heat transfer from mafic magma and attendant crustal melting.

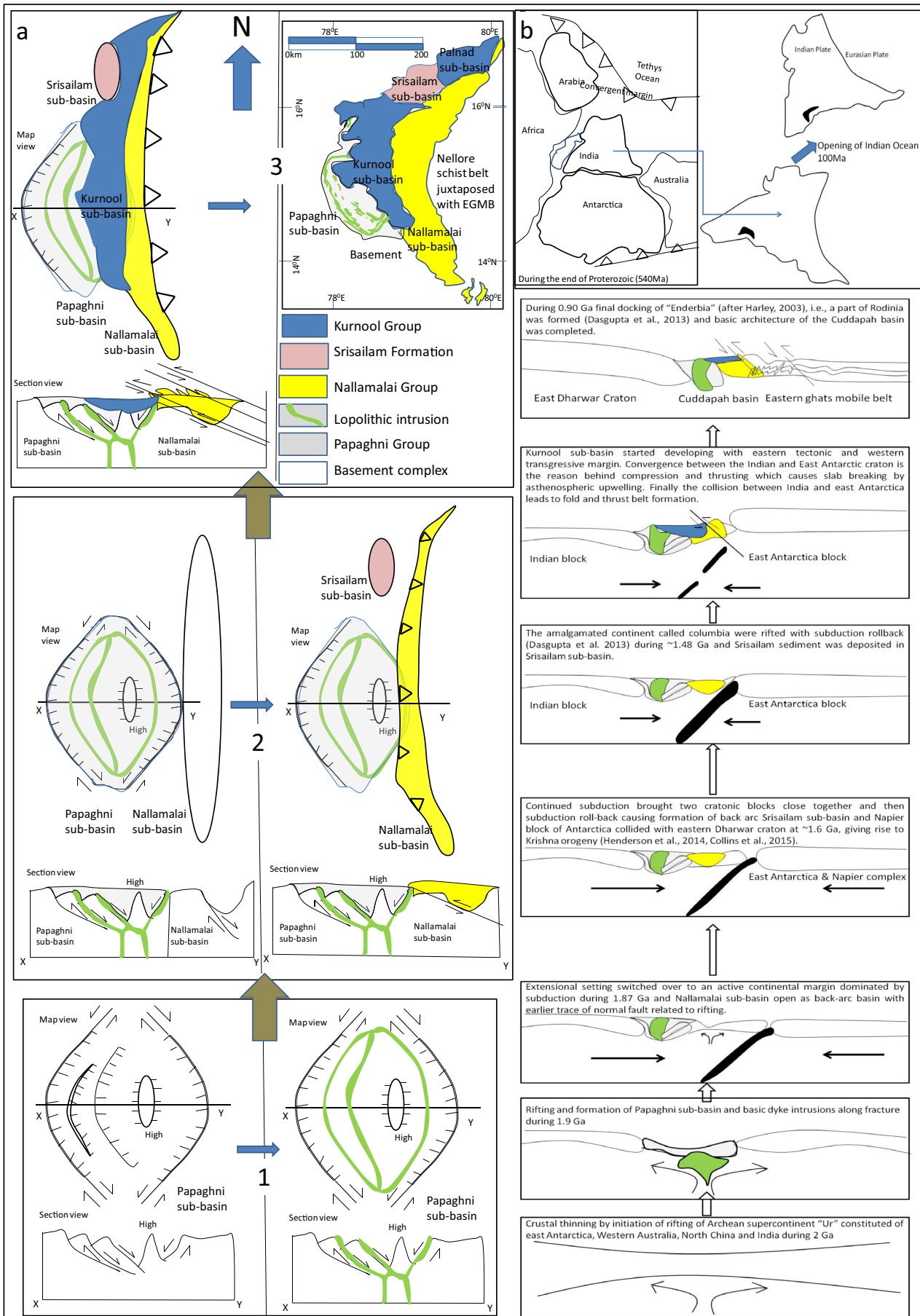
*et al.* 2014) in the vicinity of the Cuddapah basin indicate mantle plume activity and development of LIP (French *et al.* 2008). Genetic link among the five sub-basins (viz., Papaghni, Nallamalai, Srisailam, Kurnool and Palnad sub-basins) within the Cuddapah can be established with a complex history. According to Mukherjee *et al.* (2019) Papaghni Group got deposited in a rift basin associated with normal faults at the initial stage. Later, switchover to a compression regime led to development of back arc basin along earlier traces of rift related faults in the east of the Papaghni sub-basin. Such a prolonged episode of compression is related to the assembly of Columbia supercontinent. This event is related to Krishna orogeny and formation of Srisailam sub-basin as well. Kurnool sub-basin appeared during India–East Antarctica convergence.

We propose that the initially formed Papaghni sub-basin is related to active rifting during  $\sim 2$  Ga (figure 23a, b). Since, the magnitude of extensional

strain may not be uniform across the rift, more than one rift sub-basin can occur. The rift sub-basin is a portion of a rift separated from another adjacent portion by a basement high in which the crust could not be stretched as much. The combination of different rifting mechanisms, viz., stair-step faults, imbricate arrays, duplexes, rollovers, antithetic and synthetic faults may produce complex geometry of rift system (Pluijm and Marshak 2004). The extension along the entire length of a rift system does not begin everywhere coevally (Pluijm and Marshak 2004). There is a sequence of events during which rift segments link up to form a long rift system. At an early stage in rifting, segments are separated from one another along their length by the unfaulted crust. With increasing displacement on the faults in the segments, the length of the segments also increases and the individual segments interact along strike, with one dominating dip direction.

Figure 23. Tectonic model of Cuddapah basin evolution. (a) Cartoons for basin progression (1. Plan and section along X–Y showing rifting and listric normal faulting with development of depressed cup like Papaghni sub-basin and emplacement of lopoliths; 2. Further stage of sub-parallel rifting of Nallamalai sub-basin followed by sediment infilling and later smaller Srisailam sedimentation episode; 3. Thrusting and starting of eastern ghats orogenic events along with initiation of later development of Kurnool sub-basin after a short time gap. Note, that subsequent orogenic events have given rise to present shape of the basin). (b) The global plate tectonic context and its relevance to Cuddapah basin evolution (after Mukherjee *et al.* 2019).





The E–W median of the crescentic Cuddapah basin can be drawn along  $15^{\circ}10'$  in the northern part of the Papaghni sub-basin. NE–SW trending fault in north and NW–SE trending fault in south of median line is noteworthy. In the structural map of Cuddapah basin (figure 2b) this two sets of faults (viz., trending NE–SW and NW–SE) meet in the western portion of the imaginary median line. According to Saha and Tripathy (2012), the initial opening of the Cuddapah basin in the west is related to transverse faulting along these faults. The fault slip paleostress analysis suggest that stress regime in and around transverse faults during the ongoing basin opening events must have been caused by igneous activities of 1.8–1.9 Ga (Tripathy and Saha 2013). The transverse faults in the western margin of Cuddapah basin record signatures of extensional/strike-slip regime crustal deformation (Tripathy and Saha 2009; Tripathy 2011) and this may be related to rifting. Considering the explanation of Pluijm and Marshak (2004) the tip of these normal faults must have suffered a change in block movements to adjust the stress (figure 23a, phase 1). Thus the basin tapers towards the ends of the faults as the displacement on the fault changes from dip-slip in the middle to strike or oblique-slip along the terminal parts. Thus, with progressive rifting along parallel lystric normal faulting and associated lopolithic emplacements synsedimentary infilling is noteworthy (figure 23a, phase 1). Relatively later formed sub-parallel rift was the depo-centre for the Nallamalai Group. Eventually, a convergence switchover during  $\sim 1.87$  till 1.6 Ga due to Krishna orogeny (Henderson *et al.* 2014; Collins *et al.* 2015) lead to conversion of back arc basin along the earlier trace of rift related normal faulting. Therefore, such combined effects are possibly linked to Nallamalai and Srisailam sub-basins (figure 23a, phase 2). Subsequently, Kurnool sub-basin started developing with eastern tectonic and western transgressive margin. The Papaghni sub-basin with sub-elliptical lopoliths and sediments deformed later and got partially covered by younger Kurnool sediments in the eastern portion (figure 23a, phase 3). Therefore, the present day map and the section across the Papaghni sub-basin exhibit an angular unconformity between the Papaghni and Kurnool Group of rocks.

Considering the theory of Friedmann and Burbank (1995), the rifting in Cuddapah basin can be classified into a ‘supra detachment’ type in which the basin exhibit wide extended domain with

thickened crust and the master faults (i.e., detachments) are gently dipping ( $10^{\circ}$ – $30^{\circ}$ ). Unlike the ‘discrete continental rifts’, which extend slowly over long time with steep ( $45^{\circ}$ – $70^{\circ}$ ) master fault angles, the supra-detachment Cuddapah rift altogether took lesser period of extension time. The relatively longer Nallamalai basin axis could become slightly concave and fold and thrust development leads to formation of several N–S lineaments which must have given additional anisotropy and competence contrast to get curvature during subsequent orogenic events. As far as Srisailam sub-basin is concerned, this basin evolution model is partly supporting the proposal of Nagaraja Rao *et al.* (1987). Thus, with the uplift of the Nallamalai sub-basin and sinking of the basement parallel to the NE–SW lineaments resulted in the Srisailam sub-basin. Kurnool and Palnad sub-basin started developing at the end as half graben basins by subsequent tectonic reactivation. Finally, the entire system have suffered several phases of deformation during the Pan-African and Eastern Ghat orogeny and also later events of the Indian plate movements.

### Acknowledgements

We express our sincere gratitude to Shri L K Nanda, Ex-Director, AMD for encouragement and infrastructure support to publish the work. Shri V Natarajan, In-charge, Southern Cuddapah basin Investigation (SCBI), is also thankfully acknowledged. We are also thankful to all the colleagues from laboratories. Special thanks to Shri Atanu Mukherjee and Dr Soumyajit Mukherjee for the constructive comments and suggestions which helped to improve the paper significantly.

### References

- Alfe D, Gillan M J and Price G D 2003 Thermodynamics from first principles: Temperature and composition of the Earth’s core; *Mineral. Mag.* **67**(1) 113–123.
- Allen P A and Allen J R 2005 *Basin analysis*; 2nd edn, Blackwell Publishing company, ISBN 0-632-05207-4.
- Anand S P and Rajaram M 2002 Aeromagnetic data to probe the Dharwar craton; *Curr. Sci.* **83** 162–167.
- Anand M, Gibson S A, Subbarao K V, Kelley S P and Dickin A P 2003 Early Proterozoic melt generation processes beneath the intra-cratonic Cuddapah basin, southern India; *J. Petrol.* **44** 2139–2171.
- Anil Kumar, Vadlakonda P and Nagaraju E 2015 A 2082 Ma radiating dyke swarm in the Eastern Dharwar Craton,

- southern India and its implications to Cuddapah basin formation; *Precamb. Res.* **266** 490–505, <https://doi.org/10.1016/j.precamres.2015.05.039>.
- Babu Rao V, Atchuta Rao D, Ram Rao Ch, Sarma B S P, Bhaskara Rao D S, Veeraswamy K and Sarma M R L 1987 Some salient results of interpretation of aeromagnetic data over Cuddapah basin and adjoining terrain, south India; In: *Purana basins of peninsular India* (ed.) Radhakrishna B P, *Geol. Soc. India Memoir* **6** 295–312.
- Babu Rao V 1991 Geological significance of magnetic depth estimates over western part of Cuddapah basin, south India; *J. Geol. Soc. India* **38** 605–614.
- Balakrishna S and Paul P A 1970 Magnetic studies on the igneous rocks in the SW region of the Cuddapah basin and in the adjoining granitic country; IIPG Hyderabad, 2nd workshop, pp. 18–40.
- Balakrishna S, Paul P A and Ramana Rao A V 1972 Gravity and magnetic investigation in south-western region of Cuddapah basin; *Geophys. Res. Bull.* **10** 92–104.
- Balakrishna S 1979 Some recent geophysical studies in the Cuddapah basin; Proceedings of 3rd Workshop on Status, Problems and Programmes in Cuddapah basin, Hyderabad, AP, India (*Inst. Indian Penn. Geol. Publ.*), pp. 22–32.
- Bally A W, Bernoulli D, Davis G A and Montadert L 1981 Listric Normal Faults; *Oceanologica Acta. Proceedings 26th International Geological Congress*, Paris, July 7–17.
- Barberi F, Santacroe R and Varet J 1982 Chemical aspects of rift magmatism; In: *Continental and oceanic rifts* (ed.) Palmason G, Washington DC, American Geophysical Union, pp. 223–258.
- Burchardt S and Gudmundsson A 2009 The infrastructure of Geitafell Volcano, southeast Iceland; In: *Studies in Volcanology: The Legacy of George Walker* (eds) Thordarson T, Larsen G, Self S, Rowland S and Hoskuldsson A, *Geol. Soc. London, IAVCEI* **2** 349–369.
- Belica M E, Piispa E J, Meert J G, Pesonen L J, Plado J, Pandit M K, Kamenov G D and Celestino M 2014 Paleoproterozoic mafic dyke swarms from the Dharwar craton: Paleomagnetic poles for India from 2.37 to 1.88 Ga and rethinking the Columbia supercontinent; *Precamb. Res.* **244** 100–122.
- Bhaskar Rao Y J, Pantulu G V C, Damodar Reddy V and Gopalan K 1995 Time of early sedimentation and volcanism in the Proterozoic Cuddapah basin, south India: Evidence from Rb–Sr age of Pulivendla mafic sill; *Geol. Soc. India Memoir* **33** 329–338.
- Bhattacharjee P, Goswami S, Bhagat S and Verma M B 2018 Gypsum–anhydrites in 1.9 Ga Vempalle Formation, Cuddapah basin, India: A note on the Palaeoproterozoic environment and diagenetic condition; *J. Earth Syst. Sci.* **127**(8), <https://doi.org/10.1007/s12040-018-1012-6>.
- Bhattacharji S and Singh R N 1984 Thermomechanical structure of the southern part of the Indian shield and its relevance to Precambrian basin evolution; *Tectonophysics.* **105** 103–120.
- Bhattacharji S 1987 Lineaments and igneous episodes in the evolution of intracratonic Proterozoic basins on the Indian shield; In: *Geological evolution of peninsular India – petrological and structural aspects* (ed.) Saha A K, *Recent Res. Geol.* **13** 1–15.
- Bhattacharya A and Chakraborty C 2000 *Analysis of sedimentary successions: A field manual*; Oxford & IBH Publishing Co. Pvt. Ltd., New Delhi.
- Boynton W V 1984 Cosmochemistry of the rare earth elements: Meteorite studies; In: *Rare Earth Element Geochemistry* (ed.) Henderson P, Elsevier, Amsterdam, pp. 63–114.
- Brun J P 1999 Narrow rifts versus wide rifts: Inferences for the mechanics of rifting from laboratory experiments; *Phil. Trans. Roy. Soc. London Ser. A* **357** 695–712.
- Chakrabarti G, Shome D, Bauluz B and Sinha S 2009 Provenance and weathering history of mesoproterozoic clastic sedimentary rocks from the Basal Gulcheru Formation, Cuddapah basin; *J. Geol. Soc. India* **74**(7) 119–130.
- Chakraborty K, Mukhopadhyay P K and Pankaj P 2016 Magmatism in western Cuddapahs: The mafic sills and lava flows of Vempalle and Tadpatri Formations; *J. Geol. Soc. India* **87**(6) 631–660.
- Chalapathi Rao N V, Miller J A, Gibson S A, Pyle D M and Madhavan V 1999 Precise  $^{40}\text{Ar}/^{39}\text{Ar}$  dating of Kotakonda kimberlite and Chelima lamproite, India: Implication to the timing of mafic dyke swarm activity in the Eastern Dharwar craton; *J. Geol. Soc. India* **53** 425–432.
- Chandrakala K 2007 Lateral and vertical crustal velocity structure of Cuddapah basin and adjoining eastern and western Dharwar craton and seismicity of segments of peninsular India (unpublished thesis).
- Chandrakala K, Pandey O P, Mall D M and Sarkar D 2010 Seismic signatures of a Proterozoic thermal plume below south western part of Cuddapah basin, Dharwar Craton; *J. Geol. Soc. India* **76** 565–572.
- Chandrakala K, Mall D M, Dipankar S and Pandey O P 2013 Seismic imaging of the Proterozoic Cuddapah basin, south India and regional geodynamics; *Precamb. Res.* **231** 277–289.
- Chatterjee N and Bhattacharji S 2001 Petrology, geochemistry and tectonic settings of the mafic dikes and sills associated with the evolution of the Proterozoic Cuddapah basin of south India; *J. Earth Syst. Sci.* **110**(4) 433–453.
- Chaudhuri A K, Saha D, Deb G K, Patranabis-Deb S, Mukherjee M K and Ghosh G 2002 The Purana Basins of southern cratonic province of India – A case study for Mesoproterozoic fossil rifts; *Gondwana Res.* **5** 23–33.
- Collins A S, Patranabis-Deb S, Alexander E, Bertram C N, Falster G M, Gore R J, Mackintosh J, Dhang P C, Saha D, Payne J L, Jourdan F, Backé G, Halverson G P and Wade B P 2015 Detrital mineral age, radiogenic isotopic stratigraphy and tectonic significance of the Cuddapah basin, India; *Gondwana Res.* **28**(4) 1294–1309.
- Corti G 2009 Continental rift evolution: From rift initiation to incipient break-up in the Main Ethiopian Rift, East Africa; *Earth Sci. Rev.* **96** 1–53.
- Crawford A R and Compston W 1973 The age of the Cuddapah and Kurnool systems, Southern India; *J. Geol. Soc. Australia* **19**(4) 453–464.
- Das S and Chakraborty M 2017 Specialised thematic mapping of ultrapotassic volcanic rocks and associated magmatism in the Nallamalai Fold Belt of Proterozoic Cuddapah basin and their bearing on the mineralisation around Rajampata area, Cuddapah district, Andhra Pradesh; *Rec. Geol. Surv. India* **149**(5) 22–25.
- Dasgupta S and Mukherjee S 2017 Brittle shear tectonics in a narrow continental rift: Asymmetric non-volcanic Barmer basin (Rajasthan, India); *J. Geol.* **125** 561–591.
- Dasgupta P K and Biswas A 2006 *Rhythms in Proterozoic Sedimentation: An Example from Peninsular India*; Satish Serial Publishing, Delhi.

- Dasgupta S, Bose S and Das K 2013 Tectonic evolution of the Eastern Ghats Belt, India; *Precamb. Res.* **227** 247–258.
- Davis G H and Reynolds S J 1996 *Structural geology of rocks and regions* (2nd edn), John Wiley & Sons, ISBN 0-471-52621-5.
- Davis G H, Reynolds S J and Kluth C F 2012 *Structural geology of rocks and regions* (3rd edn), John Wiley & Sons, ISBN 978-0-471-15231-6.
- Deb M and Bheemalingeswara K 2008 Carbonaceous tuff-stratiform barite association in Mangampeta deposit, Andhra Pradesh, India: Implications on depositional environment and origin. Ore deposits associated with black shales from their origin to their environmental impacts: 33rd IGC, Oslo, Norway, Abstract, MRD134071.
- De La Roche H, Leterrier J, Grandclaude P and Marchal M 1980 A classification of volcanic and plutonic rocks using R1R2-diagram and major element analyses – its relationships with current nomenclature; *Chem. Geol.* **29** 183–210.
- Dewey J F and Bird J M 1970 Mountain belts and new global tectonics; *J. Geophys. Res.* **75** 2625–2647.
- Dewey J F and Hancock P L E 1987 Continental extensional tectonics; *Geol. Soc. Spec. Publ.* **28** 35–52.
- Dietz R S 1963 Collapsing continental rises, an actualistic concept of geosynclines and mountain building; *J. Geol.* **71** 314–333.
- Dutt N V B S 1975 *Geology and mineral resources of Andhra Pradesh*; Ramesh Publications, Hyderabad, 205p.
- Falvey D A 1974 The development of continental margins in plate tectonic theory; *APPEA J.* **15** 95–106.
- Fitton J G and Upton B G J 1987 Alkaline IGNEOUS ROCKS; *Geol. Soc. Spec. Publ.* **30** 568p, ISBN 0-632-061616-7.
- French J, Heaman L M, Chacko T and Srivastava R K 2008 1891–1883 Ma Southern Bastar–Cuddapah mafic igneous events, India: A newly recognized large igneous province; *Precamb. Res.* **160** 308–322.
- French E and Heaman L M 2010 Precise U/Pb dating of Paleoproterozoic mafic dyke swarms of the Dharwar Craton, India: Implications for the existence of the Neoproterozoic supercraton Sclavia; *Precamb. Res.* **183** 416–441.
- Friedmann S J and Burbank D W 1995 Rift basins and supradetachment basins: Intracontinental extensional end members; *Basin Res.* **7** 109–127.
- Geological Survey of India (GSI) 1981 Explanatory brochure on Geological and Mineral Map of Cuddapah basin, 121p.
- Gibbs A D 1983 Balanced cross-section constructions from seismic sections in areas of extensional tectonics; *J. Struct. Geol.* **5** 152–160.
- Gibbs A D 1984 Structural evolution of extensional basin margins; *J. Geol. Soc. Lond.* **141** 609–620.
- Goswami S, Vijayakumar T, Zakaulla S, Verma M B, Mohanty R and Rai A K 2012 Structural analysis of the Vempalle Fault along Samayajulapalle–Bhakrapeta tract in the Cuddapah basin, Kadapa district, Andhra Pradesh; *EARFAM* **22** 113–121.
- Goswami S, Bhattacharjee P, Bhagat S, Suresh Kumar and Zakaulla S 2015 Petrography of chert nodules in stromatolitic dolostone of Vempalle Formation, along Tummalapalle–Motnutalapalle, Cuddapah basin, India; *Indian J. Geosci.* **69** 13–24.
- Goswami S, Mukherjee A, Zakaulla S and Rai A K 2016a Stress states, faulting and their effects on the Papaghni Group, Cuddapah basin, India: A study along Giddankivaripalle–Madyalabodu tract; *Indian J. Geosci.* **70** 17–33.
- Goswami S, Sivasubramaniam R, Bhagat S, Suresh Kumar and Sarbajna C 2016b Algoma type BIF and associated submarine volcano-sedimentary sequence in Ramagiri granite-greenstone terrain, Andhra Pradesh, India; *J. Appl. Geochem.* **18**(2) 155–169.
- Goswami S, Mukherjee A, Zakaulla S and Rai A K 2016c Microbial mat related features in Palaeoproterozoic Gulcheru Formation and their role in low grade uranium mineralisation; *Int. J. Petrochem. Sci. Eng.* **1**(4) 83–89, <https://doi.org/10.15406/ipcse.2016.01.00019>.
- Goswami S, Mukherjee A, Bhattacharjee P and Zakaulla S 2017a Primary sedimentary structures and MISS in Gulcheru Quartzite along SW Part of Cuddapah basin; *J. Geol. Soc. India* **89**(5) 511–520.
- Goswami S, Bhagat S, Zakaulla S, Suresh Kumar and Rai A K 2017b Role of organic matter in uranium mineralisation in Vempalle Dolostone, Cuddapah basin, India; *J. Geol. Soc. India* **89**(2) 145–154.
- Goswami S, Upadhyay P K, Bhattacharjee P and Murugan M G 2017c Tectonic setting of the Kadiri schist belt, Andhra Pradesh, India; *Acta Geol. Sin. (English edn)* **91**(6) 1992–2006.
- Goswami S, Upadhyay P K, Bhagat S, Zakaulla S, Bhatt A K, Natarajan V and Dey S 2018 An approach of understanding acid volcanics and tuffaceous volcanoclastics from field studies: A case from Tadpatri Formation, Proterozoic Cuddapah basin, Andhra Pradesh, India; *J. Earth Syst. Sci.* **127** 20, <https://doi.org/10.1007/s12040-018-0929-0>.
- Goswami S and Dey S 2018 Facies analysis of tuffaceous volcanoclastics and felsic volcanics of Tadpatri Formation, Cuddapah basin, Andhra Pradesh, India; *Int. J. Earth Sci. (Geol. Rundsch)*, <https://doi.org/10.1007/s00531-018-1620-z>.
- Goswami S and Upadhyay P K 2019 Tectonic history of the granitoids and Kadiri Schist Belt in the SW of Cuddapah basin, Andhra Pradesh, India; In: *Tectonics and Structural Geology: Indian Context* (ed.) Mukherjee S, Springer Nature Switzerland AG 2019, Springer Geology, [https://doi.org/10.1007/978-3-319-99341-6\\_8](https://doi.org/10.1007/978-3-319-99341-6_8).
- Goswami S 2019 Lithofacies analysis and origin of felsic volcanoclastic rocks of the Palaeoproterozoic Tadpatri Formation, Cuddapah basin, southern India; Ph.D. Thesis (unpublished).
- Grant F S 1983 Results of the preliminary interpretation studies; In: Report on a visit to NGRI, Hyderabad, India – Project IND/79047, Sep–Oct 1983 (unpubl.), pp. 5–17.
- Halls H C, Kumar A, Srinivasan R and Hamilton M A 2007 Palaeomagnetic and U–Pb geochronology of easterly trending dykes in the Dharwar Craton, India: Feldspar clouding, radiating dyke swarms and the position of India at 2.37 Ga; *Precamb. Res.* **155** 47–68.
- Hargraves R B and Bhalla M S 1983 Precambrian paleomagnetism in India through 1982: A review; *Geol. Soc. India Memoir* **4** 491–524.
- Henderson B, Collins A S, Payne J, Forbes C and Saha D 2014 Geologically constraining India in Columbia: The age, isotopic provenance and geochemistry of the protoliths of the Ongole Domain, Southern Eastern Ghats, India; *Gondwana Res.* **26** 888–906.
- Hochstein M P 2005 Heat transfer by hydrothermal systems in the east African Rifts. *Proceedings World Geothermal Congress*, Antalya, Turkey, pp. 24–29.

- Illies J H 1981 Mechanism of graben formation; *Tectonophysics*. **73** 249–266.
- Irvine T N and Barager W R A 1971 A guide to the chemical classification of the common volcanic rocks; *Can. J. Earth Sci.* **8** 523–548.
- Kaila K L, Roy Chowdhury K, Reddy P R, Krishna V G, Hari Narain, Subbotin S I, Sollogub V B, Chekunov A V, Kharechko G E, Lazarenko M A and Ilchenko T V 1979 Crustal structure along Kavali–Udipi profile in the Indian peninsular shield from deep seismic sounding; *J. Geol. Soc. India* **20** 307–333.
- Kaila K L and Tewari H C 1985 Structural trends in the Cuddapah basin from deep seismic soundings (DSS) and their tectonic implication; *Tectonophysics*. **115** 69–86.
- Kaila K L, Tewari H C, Chowdhury K R, Rao V K, Sridhar A R and Mall D M 1987 Crustal structure of the northern part of the Proterozoic Cuddapah basin of India from deep seismic soundings and gravity data; *Tectonophysics*. **140** 1–12.
- Kailasam L N 1976 Geophysical studies of the major sedimentary basins of the Indian craton, their deep structural features and evolution; *Tectonophysics*. **36** 225–245.
- Kandie R J 2015 Eastern rift structural geology-tectonics, Volcanology and geothermal. Presented at Short Course X on Exploration for Geothermal Resources, organized by UNU-GTP, GDC and KenGen, at Lake Bogoria and Lake Naivasha, Kenya, Nov. 9–Dec. 1.
- Karunakaran C 1973 Barytes, Indo-Soviet Symposium on recent trends in Exploration of Minerals, Oil & Ground-water India; Nat. Sci. Acad., New Delhi.
- Karunakaran C 1976 Sulphur isotope compositions of baryte and pyrites from Mangampeta, Cuddapah district, Andhra Pradesh; *J. Geol. Soc. India* **17** 181–185.
- Keen C E 1985 The dynamics of rifting: Deformation of the lithosphere by active and passive driving mechanisms; *Geophys. J. Roy. Astron. Soc.* **80** 95–120.
- Keen C E, Courtney R C, Dehler S A and Williamson M C 1994 Decompression melting at rifted margins: Comparison of model predictions with the distribution of igneous rocks on the eastern Canadian margin; *Earth Planet. Sci. Lett.* **121**(3–4) 403–416.
- Khain V Y 1992 The role of rifting in the evolution of the Earth's crust; *Tectonophysics*. **215** 1–7.
- Kinsman D J J 1975 Rift valley basins and sedimentary history of trailing continental margins; In: *Petroleum and global tectonics* (eds) Fischer A G and Judson S, Princeton University Press, pp. 83–126.
- Kishore R K and Rama Rao C 2004 Basement characteristics of Papaghni basin of Eastern Dharwar Craton (India) – An inference from Aeromagnetic study; *J. Geophys. Union* **8**(4) 311–317.
- Koptev A, Burov E, Calais E, Leroy S, Gerya T, Laurant G F and Cloetingh S 2016 Contrasted continental rifting via plume-craton interaction: Applications to Central East African Rift; *Geosci. Front.* **7** 221–236.
- Krezsek C, Adam J and Grujic D 2007 Mechanics of fault and expulsion rollover systems developed on passive margins detached on salt: Insights from analogue modelling and optical strain monitoring; *Geol. Soc. London, Spec. Publ.* **292** 103–121, <https://doi.org/10.1144/sp292.6>.
- Krishna Brahmam N 1989 Gravity and seismicity of the Cuddapah basin and surrounding places; *J. Geol. Soc. India* **34** 373–384.
- Kumar A and Bhalla M S 1983 Paleomagnetism and igneous activity of the area adjoining the southwestern margin of the Cuddapah basin, India; *Geophys. J. Roy. Astron. Soc.* **73** 27–37.
- Lakshminarayana G, Bhattacharjee S and Ramanaidu K V 2001 Sedimentation and stratigraphic framework in the Cuddapah basin; In: National Seminar Commemorating Dr M S Krishnan's Birth centenary (Proceedings Volume), *Geol. Soc. India, Spec. Publ.* **55** 31–58.
- Le Bas M J, Le Maitre R W, Streckeisen A and Zanettin B 1986 A chemical classification of volcanic rocks based on the total alkali–silica diagram; *J. Petrol.* **27** 745–750.
- Leelanandam C 1980 Some observations on the Alkaline provinces in Andhra Pradesh; *Curr. Sci.* **50** 799–802.
- Ludwig K R 1993 ISOPLOT – A plotting and regression program for radiogenic-isotope data; version 2.70, *USGS open file report* **42** 91–445.
- Lysak S V 1987 Terrestrial heat flow of continental rifts; *Tectonophysics*. **143**(1–3) 31–41.
- Mahadevan T M 1994 Deep continental structure of India: A review; *Geol. Soc. India Memoir* **28** 569p.
- Mall D M, Pandey O P, Chandrakala K and Reddy P R 2008 Imprints of a Proterozoic tectonothermal anomaly below the 1.1 Ga kimberlitic province of southwest Cuddapah basin, Dharwar Craton (southern India); *Geophys. J. Int.* **172** 422–438.
- Manatschal G 2004 New models for evolution of magma-poor rifted margins based on a review of data and concepts from West Iberia and the Alps; *Int. J. Earth Sci.* **93** 432–466.
- Manikyamba C, Kerrich R, Alvarez I G, Mathur R and Khanna T C 2008 Geochemistry of Paleoproterozoic black shales from the intracontinental Cuddapah basin, India: Implications for provenance, tectonic setting, and weathering intensity; *Precamb. Res.* **162**(3) 424–440.
- Marle O 2011 A simple continental rift classification; *Tectonophysics*. **513** 88–95.
- Matin A 2015 Tectonics of the Cuddapah basin and a model of its evolution: A review; *Geol. Soc. London Memoir* **43**(1) 231–254.
- McKenzie D P 1978 Some remarks on the development of sedimentary basins; *Earth Planet. Sci. Lett.* **40** 25–32.
- Meijerink A M J, Rao D P and Rupke J 1984 Stratigraphic and structural development of the Precambrian Cuddapah Basin, S.E. India; *Precamb. Res.* **26** 57–104.
- Mishra D C, Laxman G, Rao M B S V and Venkatarayudu M 1985 3-Dimensional model of magnetic gravity anomalies of Cuddapah (Proterozoic) Basin, India; Technical Report, National Geophysical Research Institute (NGRI).
- Mishra D C, Baburao V, Laxman G and Rao M B S V 1987 Three-dimensional structural model of Cuddapah basin and adjacent eastern part from geophysical studies; In: *Purana Basins of Peninsular India (Middle to Late Proterozoic)* (ed.) Radhakrishna B P, *Geol. Soc. India Memoir* **6** 311–329.
- Morgan P and Baker B H E 1983 Introduction – processes of continental rifting; *Tectonophysics*. **94** 1–10.
- Mukherjee S, Goswami S and Mukherjee A 2019 Structures and their tectonic implications of the southern part of Cuddapah basin, Andhra Pradesh, India; *Iran J. Sci. Technol. Trans. Sci.* **43** 489–505.
- Murthy Y G K, Babu Rao V, Guptasarma D, Rao J M, Rao M N and Bhattacharji S 1987 Tectonic, petrochemical and

- geophysical studies of mafic dike swarms around the Proterozoic Cuddapah basin, South India; In: *Mafic dyke swarms* (eds) Halls H C and Fahrig W F, *Geol. Assoc. Canada Spec. Paper* **34** 303–316.
- Nagaraja Rao B K and Mohapatra G P 1977 Geology of Palkonda and Velikonda ranges; Progress Report for F.S. 1976–1977, *Geol. Surv. India* (unpublished).
- Nagaraja Rao B K, Rajurkar S T, Ramalingaswami G and Ravindra Babu B 1987 Stratigraphy, structure and evolution of Cuddapah basin; In: *Purana Basins of peninsular India* (ed.) Radhakrishna B P, *Geol. Soc. India Memoir* **6** 33–86.
- Neugebauer H J 1983 Mechanical aspects of continental rifting; *Tectonophysics*. **94** 1–108.
- Neumann E R and Ramberg I B 1978 *Petrology and geochemistry of continental rifts*; Reidel, Dordrecht, 296p.
- Palmason G 1982 Continental and oceanic rifts; American Geophysical Union, *Geol. Soc. Am., Geodyn. Ser.* **8**.
- Patranabis-Deb S, Saha D and Tripathy V 2012 Basin stratigraphy, sea-level fluctuations and their global tectonic connections – evidence from the Proterozoic Cuddapah basin; *Geol. J.*, <https://doi.org/10.1002/gj.1347>.
- Pluijm Van der B A and Marshak S 2004 *Earth structure: An introduction to structural geology and tectonics* (2nd edn), W. W. Norton & Company, Inc, ISBN 0-393-92467-X.
- Qureshy M N, Krishna Brahmam N, Aravamadhu P S and Naqvi S M 1968 Role of granitic intrusions in reducing the density of the crust, and other related problems as illustrated from a gravity study of the Cuddapah basin India; *Proc. Roy. Soc. London, Ser. A, Math. Phys. Sci.* **304** 449–464.
- Ramakrishnan T S 1991 Cuddapah basin configuration – another account based on gravity and aeromagnetism; *J. Geol. Soc. India* **37** 109–118.
- Ramakrishnan M and Vaidyanadhan R 2008 *Geology of India*; Vol. 1, Geological Society of India, Bangalore.
- Ram Babu H V 1993 Basement structure of the Cuddapah basin from gravity anomalies; *Tectonophysics*. **223(3–4)** 411–422.
- Ranjith M L, Santosh M, Satyanarayanan M, Subba Rao D V and Tang Li 2016 Multiple rifting and alkaline magmatism in southern India during Paleoproterozoic and Neoproterozoic; *Tectonophysics*. **680** 233–253, <https://doi.org/10.1016/j.tecto.2016.04.041>.
- Ravikant V 2010 Palaeoproterozoic (~1.9 Ga) extension and breakup along the eastern margin of the Eastern Dharwar Craton, SE India: New Sm–Nd isochron age constraints from anorogenic mafic magmatism in the Neoproterozoic Nellore greenstone belt; *J. Asian Earth Sci.* **37** 67–81.
- Reddy P R, Chandrakala K and Sridhar A R 2000 Crustal velocity structure of the Dharwar craton, India; *J. Geol. Soc. India* **55** 381–386.
- Reddy P R, Chandrakala K, Prasad A S S S R S and Rama Rao C H 2004 Lateral and vertical crustal velocity and density variations in the SW Cuddapah basin and adjoining eastern Dharwar craton; *Curr. Sci.* **87** 1607–1614.
- Rogers J J W 1993 India and Ur; *J. Geol. Soc. India* **42** 217–222.
- Ruppel C 1995 Extensional processes in continental lithosphere; *J. Geophys. Res.* **100** 24,187–24,215.
- Rychert C A, Hammond J O S, Harmon N, Kendall J M, Keir D, Ebinger C, Bastow I D, Ayele A, Belachew M and Stuart G 2012 Volcanism in the Afar Rift sustained by decompression melting with minimal plume influence; *Nature Geosci.*, <https://doi.org/10.1038/ngeo1455>.
- Saha D 2002 Multi-stage deformation in the Nallamalai fold belt, Cuddapah basin, south India – Implications for Mesoproterozoic tectonism along southeastern margin of India; *Gondwana Res.* **5** 701–719.
- Saha D, Ghosh G, Chakraborty A K and Chakraborti S 2006 Comparable Neoproterozoic sedimentary sequences in Palnad and Kurnool subbasins and their paleogeographic and tectonic implications; *Indian J. Geol.* **78** 175–192.
- Saha D and Chakraborti S 2007 Advective heat transfer and fabric development in a shallow crustal intrusive granite – the case of Proterozoic Vellaturu granite, south India; *J. Earth Syst. Sci.* **116** 433–450.
- Saha D, Chakraborti S and Tripathy V 2010 Intracontinental thrusts and inclined transpression along eastern margin of the East Dharwar Craton, India; *J. Geol. Soc. India* **75** 323–337.
- Saha D and Tripathy V 2012 Palaeoproterozoic sedimentation in the Cuddapah basin, south India and regional tectonics: A review; *Geol. Soc. London, Spec. Publ.* **365** 161–184.
- Saha D and Tripathy V 2015 Inversion of calcite twin data, paleostress reconstruction and multiphase weak deformation in cratonic interior – Evidence from the Proterozoic Cuddapah basin, India; *J. Struct. Geol.* **77** 62–81.
- Santosh M 2010 A synopsis of recent conceptual models on supercontinent tectonics in relation to mantle dynamics, life evolution and surface environment; *J. Geodyn.* **50** 116–133.
- Sarkar D, Chandrakala K, Padmavathi Devi P, Sridhar A R, Sain K and Reddy P R 2001 Crustal velocity structure of western Dharwar craton, South India; *J. Geodyn.* **31** 227–241.
- Saemundsson K 1979 Outline of the geology of Iceland; *Jökull* **29** 7–28.
- Sengör A M C and Burke K 1978 Relative timing of rifting and volcanism on Earth and its tectonic implications; *Geophys. Res. Lett.* **5** 419–421.
- Sesha Sai V V 2011 Petrology and mineral chemistry of picrite sill from Peddakudala–Velpula Area, in south-western part of the Proterozoic Cuddapah basin, Andhra Pradesh, India; In: *Dyke Swarms: Keys for Geodynamic Interpretation* (ed.) Srivastava R K, Springer Verlag, Berlin Heidelberg, pp. 115–124, ISBN-978-3-642-12496-9.
- Sesha Sai V V, Ramakrishna Reddy N, Reddy U V B, Khanna T C, Tripathy V and Ramakrishna P 2016 Field and petrological studies of the sedimentary sequence and associated mafic-felsic magmatic rocks in the Mallela section, Chitravati Group, SW part of Proterozoic Cuddapah basin, Eastern Dharwar Craton, SE India; *National Seminar on Multi-disciplinary studies on the Cuddapah basin, Andhra Pradesh and Telangana, India (Abstract)* (NMDSCB-2016), pp. 107–109.
- Sesha Sai V V, Tripathy V, Bhattacharjee S and Khanna T C 2017 Paleoproterozoic magmatism in the Cuddapah basin, India; *J. Indian Geophys. Union* **21(6)** 516–525.
- Shand S J 1943 *Eruptive Rocks. Their genesis, composition, classification, and their relation to ore-deposits with a chapter on Meteorite*; New York: John Wiley & Sons.
- Sharma M 2011 Occurrence of Neoproterozoic and Ediacaran paleobiological remains in the Purana basins of peninsular India: Implications for the age of the Kurnool, Bhima and

- Vindhyan basins. In: *National Seminar on Geodynamics and Metallogenesis of the Indian Lithosphere (Abstract Volume)*. BHU, Varanasi, 60p.
- Shelton J 1984 Listric normal faults: An illustrated summary; *Am. Assoc. Petrol. Geol. Bull.* **68**(7) 801–815.
- Sheppard S, Rasmussen B, Jian-Wei Zi, Somasekhar V, Srinivasa Sarma D, RamMohan M, Krapež B, Wilde S A and McNaughton N J 2017 Sedimentation and magmatism in the Paleoproterozoic Cuddapah basin, India: Consequences of lithospheric extension; *Gondwana Res.* **48** 153–163.
- Singh A P and Mishra D C 2002 Tectonosedimentary evolution of Cuddapah basin and Eastern Ghats mobile belt (India) as Proterozoic collision: Gravity, seismic and geodynamic constraints; *J. Geodyn.* **33** 249–267.
- Singh A P, Kumar N and Singh B 2004 Magmatic underplating beneath the Rajmahal Traps: Gravity signature and derived 3-D configuration; *Proc. Indian Acad. Sci. (Earth Planet. Sci.)* **113** 759–769.
- Subba Rao D V 2002 Zero-free air-based gravity anomaly (preliminary) map of south India – A refined and redefined Bouguer map; *Curr. Sci.* **82** 1373–1378.
- Tewari H C and Rao V K 1987 A high velocity intrusive body in the upper crust in the southwestern Cuddapah basin as delineated by deep seismic sounding and gravity modelling; In: *Purana Basins of Peninsular India*; *Geol. Soc. India Memoir* **6**.
- Thompson R N and Gibson S A 1994 Magmatic expression of lithospheric thinning across continental rifts; *Tectonophysics.* **233** 41–68.
- Tripathy V and Saha D 2009 Late structures in the Cuddapah basin, south India and its possible relation with the Gondwana assembly; In: *Asia Oceania Geosciences Society (AOGS 9)*, 11–15 August, Singapore, Asia Oceania Geosciences Society, Singapore, SE61-A006.
- Tripathy V and Saha D 2013 Plate margin paleostress variations and intracontinental deformations in the evolution of the Cuddapah basin through Proterozoic; *Precamb. Res.* **235** 107–130.
- Tripathy V, Satyapal, Mitra S K and Sesha Sai V V 2013 Fold-thrust belt architecture and structural evolution of the northern part of the Nallamalai Fold Belt, Cuddapah basin, Andhra Pradesh, India; In: *Tectonics and Structural Geology: Indian Context* (ed.) Mukherjee S, Springer Nature Switzerland AG 2019.
- Tripathy V 2011 Brittle deformation in western Cuddapah basin: Implications for Proterozoic intracontinental deformation; Unpublished Ph.D thesis, Jadavpur University.
- Venkatakrishnan R and Dotiwala F E 1987 The Cuddapah salient: A tectonic model for the Cuddapah basin, India, based on Landsat image interpretation; *Tectonophysics.* **136** 237–253.
- Veevers J J 1981 Morphotectonics of rifted continental margins in Embryo (East Africa), youth (Africa–Arabia) and maturity (Australia); *J. Geol.* **89** 57–82.
- Verma R K and Satyanarayana Y 1990 Gravity field, deep-seismic sounding and crust–mantle structure over the Cuddapah basin and Dharwar Craton of India; *Tectonophysics.* **178** 337–356.
- Walker G P L 1966 Acid volcanic rocks in Iceland; *Bull. Volcanol.* **29** 375–402.
- Wheildon J, Morgan P, Williamson K H, Evans T R and Swanberg C A 1994 Heat flow in the Kenya rift zone; *Tectonophysics.* **236**(1–4) 131–149.
- White R and McKenzie D 1989 Magmatism at rift zones: The generation of volcanic continental margins and flood basalts; *J. Geophys. Res.* **94** 7685–7729.
- Wilson M 1993 Magmatism and the geodynamics of basin formation; *Sedim. Geol.* **86** 5–29.
- Wilson B M 2007 *Igneous Petrogenesis: A Global Tectonic Approach*; Springer Science & Business Media, Chapman & Hall, Springer, 3300 AA Dordrecht, The Netherlands, 466p, ISBN-13978-0-412-53310-5 (PB).
- Winter J D 2001 *An Introduction to Igneous and Metamorphic Petrology*; Prentice Hall, Upper saddle River, New Jersey-07458, ISBN-0-13-240342-0.
- Withjack M A, Schlische R W and Olsen P E 2002 Rift-basin structure and its influence on sedimentary systems. Sedimentation in Continental Rifts; *SEPM (Society for Sedimentary Geology) Spec. Publ.* **73** 57–81, ISBN 1-56576-082-4.
- Wernicke B and Burchfield B C 1982 Modes of extensional tectonics; *J. Struct. Geol.* **4** 105–115.
- Wood D A, Joron J L, Treuil M, Norry M and Traney J 1979 Elemental and Sr isotope variations in basic lavas from Iceland and the surrounding ocean floor; *Contrib. Miner. Pet.* **70** 319–339.
- Wright T J, Ayele A, Ferguson D, Kidane T and Brown C V 2016 Magmatic rifting and active volcanism: Introduction; *Geol. Soc. London, Spec. Publ.* **420** 1–9, <http://doi.org/10.1144/SP420.18>.
- Zachariah J K, Bhaskar Rao Y J, Srinivasan R and Gopalan K 1999 Pb, Sr, Nd isotope systematic of Uranium mineralized stromatolitic dolomites from the Proterozoic Cuddapah Supergroup, South India: Constraints on age and provenance; *Chem. Geol.* **162** 49–64.
- Zhiyuan Ge, Gawthorpe R L, Rotevatn A and Thomas M B 2016 Impact of normal faulting and pre-rift salt tectonics on the structural style of salt-influenced rifts: The Late Jurassic Norwegian Central Graben, North Sea; *Basin Res.* 1–25; <https://doi.org/10.1111/bre.12219>.
- Ziegler P A 1992 Plate tectonics, plate moving mechanisms and rifting; *Tectonophysics.* **215** 9–34.